

1 **Gut Bacteria Metabolize Natural and Synthetic Steroid Hormones via the Reductive**
2 **OsrABC Pathway**
3

4 Christian Jacoby,^{1,2*} Kaylie Scorza,^{1,2*} Lia Ecker,^{1,2} Mary McMillin,¹ Ramanujam Ramaswamy,¹
5 Anitha Sundararajan,¹ Ashley M. Sidebottom,¹ Huaiying Lin,¹ Keith Dufault-Thompson,³ Brantley
6 Hall,⁴ Xiaofang Jiang,³ and Samuel H. Light^{1,2#}
7

8 ¹Duchossois Family Institute, University of Chicago, Chicago, IL, USA

9 ²Department of Microbiology, University of Chicago, Chicago, IL, USA

10 ³National Library of Medicine, National Institutes of Health, Bethesda, MD, USA

11 ⁴Department of Cell Biology and Molecular Genetics, University of Maryland, College Park,
12 College Park, MD, USA
13

14 *These authors contributed equally

15 #Address correspondence to samlight@uchicago.edu
16
17

18 **ABSTRACT**

19 Steroid hormone metabolism by the gut microbiome has multiple implications for mammalian
20 physiology, but the underlying mechanisms and broader significance of this activity remains
21 largely unknown. Here, we isolate a novel human gut bacterium, *Clostridium steroidoreducens*^T
22 strain HCS.1, that reduces cortisol, progesterone, testosterone, and related steroid hormones to
23 3 β ,5 β -tetrahydrosteroid products. Through transcriptomics and heterologous enzyme profiling,
24 we identify and biochemically characterize the *C. steroidoreducens* OsrABC reductive steroid
25 hormone pathway. OsrA is a 3-oxo- Δ^1 -steroid hormone reductase that selectively targets the Δ^1 -
26 bond present in synthetic steroid hormones, including the anti-inflammatory corticosteroids
27 prednisolone and dexamethasone. OsrB is a promiscuous 3-oxo- Δ^4 -steroid hormone reductase
28 that converts steroid hormones to 5 β -dihydrosteroid intermediates. OsrC is a 3-oxo-5 β -steroid
29 hormone oxidoreductase that reduces 5 β -intermediates to 3 β ,5 β -tetrahydro products. We find
30 that *osrA* and *osrB* homologs predict steroid hormone reductase activity in diverse gut bacteria
31 and are enriched in Crohn's disease fecal metagenomes. These studies thus identify the basis
32 of reductive steroid hormone metabolism in the gut and establish a link between inflammatory
33 disease and microbial enzymes that deplete anti-inflammatory corticosteroids.
34

35 **ACKNOWLEDGEMENTS**

36 Research reported in this publication was supported by funding from the National Institutes of
37 Health (NIGMS R35GM146969 and NIDDK P30DK042086, via the University of Chicago Center
38 for Interdisciplinary Study of Inflammatory Intestinal Disorders) and the Searle Scholars
39 Program (to S.H.L.), as well as the Deutsche Forschungsgemeinschaft (DFG, German Research
40 Foundation) – Projektnummer 542537779 (to C.J.).

41 INTRODUCTION

42 Steroid hormones encompass a broad class of biologically active molecules that play
43 crucial roles in diverse physiological processes. Corticosteroids, like cortisol, are involved in
44 regulating inflammation, immune response, and metabolism,¹ while sex steroids, including
45 estrogens, androgens, and progestins, regulate reproductive functions and secondary sexual
46 characteristics.² Due to their wide-ranging effects, both natural and synthetic steroid hormones
47 are commonly used in medical therapies to manage conditions such as autoimmune diseases,
48 hormone deficiencies, and cancers.

49 The gut microbiome mediates diverse phenotypes through the modification of host- and
50 diet-derived metabolites, including various steroids. Research on microbiome steroid
51 metabolism has primarily focused on bile acids, products of which are important for multiple host
52 phenotypes.³⁻⁵ However, while less studied, steroid hormones have also been identified as an
53 important class of substrates in the gut. These molecules interact with gut microbes after
54 entering the gastrointestinal tract via therapeutic oral or rectal administration or through
55 excretion in bile.⁶ Bile is likely a particularly important source of intestinal steroid hormones, as
56 9-22% of endogenous cortisol,^{7,8} 10-15% of testosterone,⁹ 20-30% of corticosterone,¹⁰ and up to
57 30% of progesterone¹¹ are eliminated from the body through this route.

58 Gut microbes generate multiple products from steroid hormones, including cortisol and
59 corticosterone derivatives that serve as fecal biomarkers for stress in animal research
60 studies.^{12,13} In addition to passing into feces, intestinal microbial steroid hormone products can
61 reenter the bloodstream through enterohepatic circulation. In humans, this is evidenced by the
62 rectal administration of cortisol leading to an increase in specific circulating cortisol derivatives
63 in a microbiome-dependent manner.^{14,15} Other studies provide evidence that microbial products
64 of progesterone metabolism similarly enter systemic circulation.^{6,16}

65 The impact of microbial steroid hormone metabolism has been linked to several aspects
66 of mammalian biology. Microbial inactivation of orally administered steroids, including side-chain
67 cleavage of synthetic corticosteroids, reduces the bioavailability of these drugs.^{17,18} Microbial
68 pathways that dehydroxylate corticosterone and convert steroid precursors to androgens
69 generate metabolites that contribute to hypertension in animal models^{19,20} and promote
70 castration-resistant prostate cancer,^{21,22} respectively. Bacterial metabolisms that alter the
71 concentration of steroid hormones with distinct biological activities thus have diverse
72 consequences for mammalian biology.

73 Previous studies have reported that some gut bacteria reduce the Δ^4 -bond in steroid
74 hormones, generating 5β -steroid derivatives.²³ This activity decreases the anti-inflammatory and
75 androgenic properties of glucocorticoids and androgens, respectively, and converts progestins
76 into a neuroactive form.²⁴ While it stands to reason that Δ^4 -steroid hormone reduction may have
77 implications for host biology, the molecular basis and the broader significance of activities in the
78 gut microbiome remains unknown.

79 Here, we describe the isolation and characterization of a novel steroid hormone-
80 metabolizing gut bacterium, *Clostridium steroidoreducens* HCS.1. By employing a
81 multidisciplinary approach, integrating genomics, transcriptomics, and metabolomics, we
82 characterize the *osrABC* reductive steroid hormone pathway. These findings provide new
83 insights into the diversity of steroid hormone metabolism in the gut microbiome and its potential
84 impact on host health.

85 RESULTS

87 *Clostridium steroidoreducens* is a novel steroid hormone-enriched gut bacterium

88 To select for members of the gut microbiome with metabolic capabilities that provide a
89 selective advantage in the presence of steroid hormones, we passaged a human fecal sample
90 in a nutritionally limited base medium supplemented with individual corticosteroids (cortisol or
91 corticosterone) or sex steroids (progesterone or testosterone) (**Figure 1A**). We isolated strains

92 from the final enrichment passages and cultivated them on steroid hormone-infused solid
93 media. We identified one strain, HCS.1, that cleared insoluble cortisol or progesterone from the
94 solid media and accumulated a white precipitate indicative of a potential reaction product at
95 colony centers on progesterone-infused media (**Figure 1B and 1C**). Consistent with HCS.1
96 possessing a selective advantage in the presence of steroid hormones, 16S rRNA amplicon
97 sequencing of the final enrichment passages revealed an amplicon sequence variant matching
98 the HCS.1 16S rRNA sequence was enriched from below the limit of detection in the fecal
99 inoculum to 0.7-23.6% of the microbial community following cortisol, corticosterone,
100 progesterone, or testosterone enrichment (**Figure 1D**).

101 To facilitate further strain characterization, we sequenced and assembled HCS.1 DNA
102 into 3 circularized contigs, comprising a genome and two plasmids, that contain 3,816,008 base
103 pairs with 28.4% G + C content, 3595 protein-coding genes, and 111 RNA genes (**Figure 1E**).
104 Phylogenetic analyses revealed that HCS.1 was closely related to *Clostridium chrysemydis* but
105 represents a novel species of the genus *Clostridium*, based on an average nucleotide identity
106 (ANI) of 92.09% to the closest reference genome and accepted taxonomic assignment criteria
107 (**Extended Data Figure 1**).²⁵ In recognition of steroid hormone reductase activities detailed
108 below, we assigned HCS.1 the species name *Clostridium steroidoreducens*.

109

110 **C. steroidoreducens possesses broad steroid hormone reductase activity**

111 To determine whether the *C. steroidoreducens* HCS.1 steroid clearance phenotype was
112 indicative of metabolic activity, we employed an LC-MS-based assay to track the fate of cortisol
113 or progesterone in *C. steroidoreducens* HCS.1 culture. We observed that both steroid hormones
114 were fully depleted from the media, coinciding with the emergence of a minor and major
115 product. By comparing to compound reference standards, we confirmed that major and minor
116 products corresponded to 5 β -dihydro- and 3 β ,5 β -tetrahydro-steroid derivatives, respectively
117 (**Figure 2A, Extended Data Figure 2**).

118 Tracking *C. steroidoreducens* HCS.1 cortisol metabolism over time, we observed that
119 5 β -dihydrocortisol transiently accumulated, peaking at 60 minutes before decreasing to less
120 than 2% of the total corticosteroid present by 120 minutes (**Figure 2B**). By contrast, 3 β ,5 β -
121 tetrahydrocortisol steadily accumulated following the introduction of cortisol, exceeding 98% of
122 the corticosteroid present by 120 minutes (**Figure 2B**). These results suggest that, in contrast to
123 previously characterized bacterial steroid dehydroxylation²⁶ and side chain-cleaving²⁷ activities,
124 *C. steroidoreducens* HCS.1 exclusively reduces cortisol, converting it to 3 β ,5 β -tetrahydrocortisol
125 via a 5 β -dihydrosteroid intermediate (**Figure 2C**).

126 To address the specificity of *C. steroidoreducens* HCS.1 steroid utilization, we next
127 tested the strain's activity on a panel of steroids with variable functional groups at multiple
128 positions on the sterol core (**Figure 2D**). We found that *C. steroidoreducens* tolerated
129 substitutions at C1, C11, C17 positions, exhibiting activity on distinct corticosteroids
130 (corticosterone, cortisone, prednisolone) and sex steroids (progesterone, testosterone) (**Figure**
131 **2E**). In contrast to these polar steroids, the hydrophobic cholesterol-derivative cholestenone
132 was a poor substrate (**Figure 2E**). These results establish *C. steroidoreducens* as a steroid
133 hormone-reducing gut bacterium with broad substrate specificity.

134

135 **Fe-S flavoenzyme family OsrB is a 3-oxo- Δ^4 -steroid hormone reductase**

136 We next sought to identify the mechanism of steroid hormone reduction by *C.*
137 *steroidoreducens*. As bacterial reductases are often induced in the presence of their
138 substrate,^{26,28} we employed a transcriptomics-based approach to identify candidate steroid
139 hormone reductases in *C. steroidoreducens*. We performed RNA-seq analysis on *C.*
140 *steroidoreducens* cells cultivated in the presence or absence of cortisol and identified 30 genes
141 that were induced >2-fold when cortisol was present (**Supplementary Table 1**). Two of the most
142 highly induced genes, which we renamed *osrA* and *osrB* (oxosteroid reductase A and B),

143 encoded proteins annotated as *fadH*-like 2,4-dienoyl-CoA reductases (**Figure 3A,**
144 **Supplementary Table 1**).

145 *E. coli* 2,4-dienoyl-CoA reductase is the best characterized member of the “Fe-S
146 flavoenzyme family” of oxidoreductases that contain a conserved N-terminal substrate-binding
147 domain (PF00724) and a C-terminal NAD(P)H cofactor-binding domain (PF07992) (**Figure**
148 **3B**).²⁹ Divergent members of the Fe-S flavoenzyme family are widespread in gut bacteria and
149 possess distinct substrate specificities for host- and diet-derived metabolites.³⁰ Consistent with
150 OsrA and OsrB representing novel Fe-S flavoenzyme subtypes with distinct substrates, we
151 observed that these enzymes exhibited remote sequence homology to previously characterized
152 Fe-S flavoenzymes, including *Clostridium scindens* Fe-S flavoenzymes, BaiCD and BaiH, which
153 reduce bile acid intermediates structurally related to steroid hormones (**Figure 3C**).^{29,31}

154 To test steroid reductase activity of OsrA and OsrB, we heterologously produced the
155 enzymes in anaerobically cultured *E. coli* cells. We found cells expressing *osrB*, but not *osrA*,
156 reduced cortisol to 5 β -dihydrocortisol (**Figure 3D**). Studies with anaerobically purified OsrB
157 revealed that NADH and NADPH were poor electron donors for OsrB. Using the artificial
158 electron donor methyl viologen, we observed that OsrB similarly reduced a variety of steroid
159 hormones substrates (**Figure 3E**). These results thus establish OsrB as a promiscuous 3-oxo-
160 Δ 4-steroid hormone reductase that uses a presently unidentified electron donor.

161
162 **Short chain dehydrogenase OsrC is a 3-oxo-5 β -steroid hormone oxidoreductase**

163 We next sought to identify the *C. steroidoreducens* enzyme responsible for reduction
164 of the 3-oxo group on the 5 β -dihydrosteroid intermediate generated by OsrB. Microbial bile
165 acid oxidoreductases with specificity for 3 α -, 3 β -, 7 α -, 7 β -, 12 α - and 12 β -hydroxyl groups
166 have been previously identified.³²⁻³⁴ As these characterized steroid oxidoreductases are
167 members of the short chain dehydrogenase (SDR) enzyme superfamily, we reasoned the *C.*
168 *steroidoreducens* enzyme was likely related to this family. An analysis of the *C.*
169 *steroidoreducens* genome identified 12 genes with SDR domains. However, none were
170 induced by cortisol or exhibited high sequence similarity to previously characterized bile acid
171 oxidoreductases.

172 As these analyses failed to identify obvious candidates, we next performed an
173 unbiased screen of SDR-containing *C. steroidoreducens* proteins for 3-oxo-5 β -steroid
174 hormone reductase activity. We confirmed soluble expression of all 12 SDRs in *E. coli* and
175 tested the activity of overexpressing *E. coli* strains on 5 β -dihydrocortisol (**Figure 4A,**
176 **Extended Data Figure 3**). We identified two SDRs (BLEONJ_2554 and BLEONJ_1088) that
177 produced 3 β ,5 β -tetrahydrocortisol and two others (BLEONJ_2478 and BLEONJ_1414) that
178 yielded 3 α ,5 β -tetrahydrocortisol (**Figure 4A**).

179 Studies with anaerobically purified BLEONJ_2554 and BLEONJ_1088 revealed
180 divergent substrate specificities. BLEONJ_2554 showed a pronounced preference for 5 α -
181 steroids and exhibited weak activity that did not follow classical Michaelis-Menten kinetics with
182 5 β -steroid substrates (**Figure 4B, Extended Data Figure 4**). Conversely, gene BLEONJ_1088
183 displayed a preference for 5 β -steroid hormones and accommodated multiple functional groups
184 at the C9 or C17 positions (**Figure 4B, Extended Data Figure 5**). We further found that
185 BLEONJ_1088 exhibited a preference for steroid hormones relative to the comparable bile acid
186 derivative lithocholic acid. We thus conclude that BLEONJ_1088 is a 3-oxo- Δ ⁴-steroid hormone
187 reductase and, on this basis, renamed it OsrC.

188
189 **Fe-S flavoenzyme family OsrA is a 3-oxo- Δ ¹-steroid hormone reductase active on**
190 **synthetic corticosteroids**

191 Synthetic corticosteroids possess potent anti-inflammatory properties and are used to
192 treat a range of pathologies, including inflammatory bowel disease.³⁵ The synthetic
193 corticosteroids drugs dexamethasone, prednisone, prednisolone, and methylprednisolone

194 contain a Δ^1 -bond that is absent in natural corticosteroids and which significantly extends their
195 half-life (**Figure 5A**).³⁶ As our initial screen of steroids identified prednisolone as a substrate for
196 *C. steroidoreducens* (**Figure 1**), we sought to address the molecular basis of synthetic
197 corticosteroid metabolism. We first tested *C. steroidoreducens* activity on additional synthetic
198 corticosteroids dexamethasone, prednisone, and methylprednisolone and found that all were
199 reduced to $3\beta,5\beta$ -tetrahydrocortisol derivatives, indicating that the bacterium possesses both Δ^1 -
200 and Δ^4 -steroid hormone reductase activities (**Figure 5B**).

201 Considering the similarity of the Δ^1 -reduction to the OsrB catalyzed Δ^4 -reduction, we next
202 tested the activity of OsrA and OsrB and found that the two enzymes generated distinct cortisol
203 and testosterone isomers from prednisolone and the synthetic androgen boldenone,
204 respectively (**Figure 5C, Extended Data Figure 6**). Based on comparison to reference
205 standards, we establish that OsrA and OsrB products reflected Δ^1 - and Δ^4 -steroid hormone
206 reductase activities, respectively (**Extended Data Figure 6**). These results demonstrate that
207 OsrA functions as a Δ^1 -steroid hormone reductase that acts in conjunction with OsrB and OsrC
208 to reduce synthetic steroid hormones to $3\beta,5\beta$ -reduced products (**Figure 5E**).

209 **Steroid hormone reductase activities are common in gut bacteria and correlate with the** 210 **distribution of *osrA* and *osrB* homologs**

211 We next sought to address the breadth of steroid hormone reductase activity in the gut
212 microbiome. We performed BLASTp searches of OsrA, OsrB, and OsrC in the Unified Human
213 Gastrointestinal Genome catalog of representative genomes and metagenome-assembled
214 genomes, which includes 4,644 prokaryotic species that colonize the human gastrointestinal
215 tract.³⁷ These searches identified homologs with high sequence homology to OsrA, OsrB, and
216 OsrC in 2, 59, and 90 genomes, respectively (**Supplementary Table 2**). Genomes encoding
217 *osrABC* homologs included gram-positive bacterial species from multiple taxa, primarily from the
218 Erysipelotrichaceae and Lachnospiraceae families.

219 To determine the association of *osrABC* homologs with observed *C. steroidoreducens*
220 phenotypes, we selected 117 gut bacteria strains for experimental characterization. We tested
221 these strains on solid media on steroid clearance/precipitate accumulation and assayed a select
222 subset for cortisol and prednisolone activity. From these studies we identified 29 strains from 14
223 species with a steroid clearance/precipitate accumulation phenotype and 6 species isolates with
224 steroid hormone reductase activity (**Figure 6A-6C and Supplementary Table 3**).

225 Comparing strain genotypes to observed phenotypes revealed several patterns. First,
226 presence of an *osrB* homolog in a genome strongly predicted steroid clearance/precipitate
227 accumulation and steroid hormone Δ^4 -reductase activity (**Figure 6B and Supplementary Table**
228 **3**). Second, the absence of *osrA* homologs tracked with a consistent lack of steroid hormone Δ^1 -
229 reductase activity (**Figure 6C and Supplementary Table 3**). Third, while the presence of an
230 *osrC* homolog tracked with production of $3\beta,5\beta$ -tetrahydrocortisol, absence of an *osrC* homolog
231 was not predictive of fate of the C3 functional group. Indeed, *osrC*-negative strains varied in
232 their major cortisol product, generating either 5β -dihydrocortisol, $3\alpha,5\beta$ -tetrahydrocortisol, or
233 $3\beta,5\beta$ -tetrahydrocortisol (**Figure 6B and Supplementary Table 3**). These results provide
234 evidence that *osrA* and *osrB* specifically confer Δ^1 - and Δ^4 -steroid hormone reductase activities,
235 respectively, while *osrC* likely represents one of multiple evolutionarily distinct 3-oxo- 5β -steroid
236 hormone oxidoreductases.

237 ***osrB* is prevalent in human fecal metagenomes and associated with active Crohn's** 238 **disease**

239 Having established the relevance of *osrABC* homologs for steroid reductase activity in
240 gut bacteria, we next sought to determine the prevalence of the pathway in the human gut. We
241 focused our analysis on *osrA* and *osrB*, since these homologs reliably predicted steroid
242 hormone reductase activities of assayed strains. We recruited reads to *osrA* and *osrB* homologs
243
244

245 in a collection of 1,491 previously published healthy human fecal metagenomes. We detected at
246 least one read mapping to *osrA* and *osrB* homologs in 2.2% and >98.9% of samples,
247 respectively (**Supplementary Table 4**). Within most metagenomes multiple *osrB* homologs
248 recruited many reads. By contrast, the majority *osrA* reads recruited to *Clostridium tertium osrA*
249 homologs, often with only one or two reads per metagenome (**Supplementary Table 4**). These
250 analyses demonstrate that *osrB* homologs are common in the gut but that *osrA* homologs are
251 confined to bacteria that colonize the gut at a low relative abundance.

252 Considering that glucocorticoids possess potent anti-inflammatory activities and natural
253 and synthetic variants, including cortisol and prednisolone, are rectally and orally administered
254 for the treatment of inflammatory bowel disease, we reasoned that OsrA and OsrB activity could
255 be clinically relevant in this patient population. We analyzed 314 metagenomes from the Lewis
256 et al.³⁸ study of active Crohn's disease patients, including a subset treated with corticosteroids
257 (**Supplementary Table 5**). We observed *osrB* homologs were elevated in Crohn's disease
258 patient relative to a healthy control population (**Figure 6D**). Further scrutiny revealed that the
259 increased abundance *osrB* homologs from *Ruminococcus_B gnavus* and *Clostridium_AQ*
260 *innocuum*, two taxa previously associated with Crohn's disease inflammation,^{39,40} was the
261 primary driver of this association (**Figure 6E**).

262 *osrA* homologs similarly exhibited elevated abundance in Crohn's disease
263 metagenomes, but their low prevalence coupled with the relatively small sample size of this
264 dataset complicated statistical analysis of the significance of this relationship (**Figure 6D**). To
265 address this issue, we expanded our dataset to include 1537 metagenomes from multiple
266 separate studies that included Crohn's disease and control populations. Analysis of this larger
267 dataset confirmed that *osrA* homologs were significantly elevated in Crohn's disease patient
268 metagenomes and revealed that the *osrA* from *Clostridium tertium* was the primary driver of this
269 association (**Extended Data Figure 7A and 7B, Supplementary Table 5**).

270 To determine whether identified associations extended an independent dataset, we
271 evaluated 569 Crohn's disease patient metagenomes collected as part of Integrative Human
272 Microbiome Project (**Supplementary Table 6**). We observed a similar association between
273 elevated abundance of *osrA* and *osrB* homologs and microbiome dysbiosis scores used as a
274 proxy for active Crohn's disease in this study (**Extended Data Figure 8A-8C, Supplementary**
275 **Table 6**).⁴¹ Underscoring the relevance of these observations to active Crohn's disease,
276 metagenomes from this study with microbiome dysbiosis score consistent with inactive Crohn's
277 disease exhibited intermediate *osrB* homolog levels between dysbiotic Crohn's disease and
278 control non-IBD populations (**Extended Data Figure 8A, Supplementary Table 6**).

279 We further investigated the relationship between microbial steroid reductases and
280 corticosteroid treatment in Crohn's disease patients, as reported in the Lewis et al.³⁸ study. Our
281 analysis revealed that corticosteroid therapy was associated with an increase in *osrA* homolog
282 prevalence, as these homologs were detected in 9.6% of corticosteroid-treated patients
283 compared to only 2.4% in untreated patients. This suggests a potential selective pressure
284 favoring bacteria that metabolize synthetic corticosteroids in patients receiving these therapies.
285 Interestingly, within the metagenomes where *osrA* homologs were present, their abundance did
286 not significantly differ between treated and untreated patients, suggesting that the effect of
287 corticosteroid treatment may relate to increased colonization of bacteria with *osrA* homologs
288 (**Extended Data Figure 9**).

289 **DISCUSSION**

291 In this study, we characterize *Clostridium steroidoreducens* HCS.1, a previously
292 uncharacterized gut bacterium that encodes a novel reductive pathway, OsrABC, for the
293 metabolism of steroid hormones. Our work expands on previous studies of microbial steroid
294 metabolism by demonstrating the widespread prevalence and activity of OsrB and OsrC in the
295 gut microbiota, which catalyze the reduction of natural steroid hormones into their 3 β 5 β -

296 tetrahydro derivatives. Notably, the OsrB homologs are prevalent in Crohn's disease-associated
297 bacterial communities, implicating these enzymes in both health and disease contexts.

298 One of the most compelling aspects of this work is the link between microbial steroid
299 metabolism and chronic inflammatory conditions, particularly Crohn's disease. Our data indicate
300 that *osrB* homologs are enriched in pro-inflammatory taxa such as *Clostridium_AQ innocuum* and
301 *Ruminococcus_B gnavus*, both of which have previously been associated with Crohn's
302 disease.^{39,40} Pro-inflammatory gut microbes often exhibit a competitive advantage in
303 inflammatory conditions and induce inflammation to generate conditions favorable for their
304 growth.⁴¹ This suggests that these microbes may leverage steroid hormone metabolism to gain
305 a competitive advantage in the inflamed gut environment. Specifically, OsrB-mediated depletion
306 of endogenous anti-inflammatory glucocorticoids may represent an adaptive strategy employed
307 by *Clostridium_AQ innocuum* and *Ruminococcus_B gnavus* to perpetuate inflammation and
308 support their growth.

309 In a clinical context, the OsrABC reductase pathway may also have significant
310 implications for glucocorticoid therapies, which are commonly administered to manage
311 inflammatory bowel disease. Our findings suggest that the OsrABC reductase pathway could
312 modulate the effective dose of administered glucocorticoids by degrading these anti-
313 inflammatory compounds. This underscores the importance of further investigations into the
314 microbial impact on drug bioavailability in relation to both the efficacy and dosing of steroid
315 therapies in patients.

316 Beyond the clinical considerations, our study highlights the broader significance of gut
317 microbial steroid metabolism in human health. Notably, a concurrently published manuscript
318 independently identifies the 3-oxo- Δ^4 -steroid hormone reductase activity of OsrB homologs,
319 along with the characterization of additional novel gut bacterial enzymes that metabolize
320 progestins.⁴² Together, these findings represent a crucial step forward in delineating the broader
321 landscape of microbial steroid hormone metabolism and its potential clinical implications.

322
323

324 **MATERIALS AND METHODS**

325 Steroid hormone enrichment culture

326 For each enrichment sample, 15 mM steroid hormone (cortisol, corticosterone,
327 progesterone, or testosterone) suspensions were prepared in 1 mL basal growth medium (Difco
328 M9 minimal salts, 20 mM acetate, 20 mM formate, tryptone 0.01% w/v, Bacto yeast extract
329 0.01% w/v, trace vitamins and minerals, MgSO₄ 4.09% w/v; pH 6.5). Homogenized fecal
330 samples were pelleted and washed 3x in phosphate buffer saline (PBS), then resuspended in 1
331 mL saline. 20 μ L cell suspension was added to each enrichment culture condition and incubated
332 for 72 hours. After 72 hours, 20 μ L of each culture was used to inoculate fresh media
333 supplemented with its respective compound. Cultures were passaged a total of 4 times. After
334 the final passage, a portion of each condition was preserved in 20% glycerol and frozen at -80
335 °C. The remaining culture was pelleted and processed for 16S rRNA sequencing.

336

337 Isolation of HCS.1

338 Preserved stocks of enrichment culture samples were plated onto fresh brain heart
339 infusion (BHI) agar and incubated for 4 days at 37 °C under anaerobic conditions (5% H₂, 10%
340 CO₂, 85% N₂). Distinct colonies were passaged to confirm purity and identified by 16S rRNA V4-
341 V5 variable region sequencing. Purified isolates of HCS.1 were stored at -80 °C in a 20%
342 glycerol suspension. Frozen glycerol stocks were deposited in the DFI Symbiotic Bacterial
343 Strain Bank Repository (<https://dfi.cri.uchicago.edu/biobank/>).

344

345 Steroid clearance assay

346 To prepare steroid clearance assays, progesterone and cortisol amounts for a final
347 concentration of 12 mM or 16 mM, respectively, were sterilized by suspension in 70% v/v
348 ethanol, followed evaporation at room temperature for 2 hours. Dried steroid powders were
349 sifted into autoclaved BHI agar and stirred rapidly, shortly before pouring into plates. Solid
350 plates were stored under anaerobic conditions at 25 °C for at least 24 hours prior to use.

351 To test HCS.1 steroid clearance, solid BHI plates were incubated at 37 °C for 2 days.
352 After 2 days, single colonies were picked and suspended in 200 µL PBS. Aliquots of the cell
353 suspension were spread onto solid steroid plates and incubated anaerobically for 5 days at 37
354 °C. To test steroid clearance of other bacterial strains, solid BHI plates were incubated at 37 °C
355 for 4 days. After 4 days, single colonies from each isolate were picked and suspended in 200 µL
356 PBS. 2 µL aliquots were spotted onto solid progesterone plates, dried, and incubated
357 anaerobically for 3 days at 37 °C.

358 359 16S rRNA sequencing and analysis

360 Cells from final steroid enrichment passages were collected by centrifugation and their
361 genomic DNA extracted using the QIAamp PowerFecal Pro DNA kit (Qiagen). Briefly, samples
362 were suspended in a bead tube (Qiagen) along with lysis buffer and loaded on a bead mill
363 homogenizer (Fisherbrand). Samples were then centrifuged, and the supernatant was
364 resuspended in a reagent that effectively removed inhibitors. DNA was then purified routinely
365 using a spin column filter membrane and quantified using Qubit. The 16S rRNA variable V4-V5
366 region was amplified using universal bacterial primers, 564F and 926R. Amplicons were purified
367 using magnetic beads, then quantified and pooled at equimolar concentrations. The Qiagen
368 QIAseq one-step amplicon library kit was used to ligate Illumina sequencing-compatible
369 adaptors onto amplicons. Reads were sequenced on an Illumina MiSeq platform to generate 2 x
370 250 base pair reads, with 5,000-10,000 reads per sample. Amplified 16S rRNA amplicons were
371 processed through the dada1 pipeline in R. Forward reads were trimmed at 210 bp and reverse
372 reads were trimmed at 150 bp, to remove low-quality nucleotides. Chimeras were detected and
373 removed using default parameters. Amplicon sequence variants between 300 and 360 bp in
374 length were taxonomically assigned to the genus level using the RDP Classifier (v2.13) with a
375 minimum bootstrap confidence score of 80.

376 377 Sample preparation for whole genome sequencing

378 To prepare HCS.1 for whole genome sequencing, 10 mL BHI broth was inoculated with
379 cells from a single bacterial colony and incubated anaerobically at 37 °C for 48 hours. The
380 culture was centrifuged at 4000 x g for 10 minutes. The resulting pellet was resuspended,
381 washed in phosphate buffer saline (PBS), and re-centrifuged.

382 383 Whole genome sequencing library preparation: Illumina short reads

384 Samples for Illumina short sequencing were extracted using the QIAamp PowerFecal
385 Pro DNA kit (Qiagen), as described in the preceding subsection. Libraries were prepared using
386 200 ng of genomic DNA using the QIAseq FX DNA library kit (Qiagen). Briefly, DNA was
387 fragmented enzymatically into shorter fragments and desired insert size was achieved by
388 adjusting fragmentation conditions. Fragmented DNA was end repaired and 'A's' were added to
389 the 3'ends to stage inserts for ligation. During ligation step, Illumina compatible Unique Dual
390 Index (UDI) adapters were added to the inserts and prepared library was PCR amplified.
391 Amplified libraries were cleaned up, and QC was performed using TapeStation 4200 (Agilent
392 Technologies). Libraries were sequenced on an Illumina NextSeq 1000/2000 to generate
393 2x150bp reads.

394 395 Whole genome sequencing library preparation: Oxford Nanopore long reads

396 Samples for Nanopore and Illumina hybrid assemblies were extracted using the high
397 molecular weight NEB Monarch Genomic DNA Purification Kit. DNA was QC'ed using genomic
398 Tapestation 4200. Nanopore libraries were prepared using the Rapid Sequencing Kit (SQK-
399 RAD114) and sequenced on MinION R10.4.1 flow cells. Nanopore reads were base-called
400 using ONT Guppy basecalling software version 6.5.7+ca6d6af, minimap2 version 2.24-r1122,
401 and was demultiplexed using ONT Guppy barcoding software version 6.5.7+ca6d6af using local
402 HPC GPU. N50 of the nanopore long read is 7077 base pairs, the average read length is 4529.4
403 base pairs, while the average read quality is 15.6, which is typical of Nanopore reads. Hybrid
404 assembly was performed with both nanopore and Illumina short reads using Unicycler
405 v0.5.0.^{43,44}

407 Taxonomic classification of *Clostridium steroidoreducens* sp. nov. Strain HCS.1^{AT}

408 The classification of strain HCS.1 as a novel species, *Clostridium steroidoreducens* sp.
409 nov. was performed using GTDB-Tk (version 2.3.2)⁴⁵ on the KBase platform. Genome quality
410 assessment, phylogenetic placement, and taxonomic classification were performed according to
411 GTDB guidelines. The HCS.1 genome was uploaded to the KBase website and analyzed using
412 the GTDB-Tk classify workflow, which assigns genomes to the closest known taxa based on
413 conserved marker genes. Strain HCS.1 was classified within the genus *Clostridium*, but did not
414 match any known species in the Genome Taxonomy Database (GTDB, version r207).
415 Phylogenetic placement within the GTDB bacterial tree confirmed that the strain represented a
416 distinct lineage, supporting its designation as a new species.

418 Transcriptomic analysis of HCS.1

419 To prepare HCS.1 samples for transcriptomic analysis, six 50 mL Lysogeny broth
420 cultures were inoculated with bacteria cells and shaken anaerobically at 37 °C for 48 hours. After
421 48 hours, cortisol powder was added to 3 cultures, to a final concentration of 8 mM. All 6
422 cultures were incubated for an additional 4 hours, then pelleted at 4000 x g for 10 minutes. The
423 resulting pellets were flash-frozen in a dry ice/ethanol bath and stored at -80 °C until ready for
424 subsequent processing. Cell pellets were thawed and total RNA from biological replicates
425 extracted using the Maxwell RSC instrument (Promega). Extracted RNA was quantified using
426 Qubit, and integrity was measured using TapeStation (Agilent Technologies). Libraries from ribo-
427 depleted samples were constructed using the NEB's Ultra Directional RNA library prep kit for
428 Illumina. First, up to 500 ng total RNA was subjected to ribosomal RNA depletion (for bacteria)
429 using NEBNext rRNA depletion kit. Ribosomal -RNA depleted samples were fragmented based
430 on RNA integrity number (RIN). Post cDNA synthesis, Illumina compatible adapters were ligated
431 onto the inserts and final libraries were QC'ed using TapeStation (Agilent technologies).
432 Libraries were normalized using library size and final library concentration (as determined by
433 Qubit). Library concentration (ng/ul) was converted to nM to calculate dsDNA library
434 concentration. Equimolar libraries were then pooled together at identical volumes to ensure
435 even read distribution across all samples. Normalized libraries were then sequenced on
436 Illumina's NextSeq 1000/2000 at 2x100bp read length.

437 High-quality reads were mapped to the circularized hybrid assembled genome of HCS.1
438 (NCBI: CP170704), using Bowtie2 (v.2.4.5), and sorted with Samtools (v1.6). Read counts were
439 generated using featureCounts (v2.0.1) with Bakta annotations.⁴⁶ Gene expression was
440 quantified as the total number of reads uniquely aligning to the reference genome, binned by
441 annotated gene coordinates. Differential gene expression and quality control analyses were
442 performed using DESeq2 in R with Benjamini-Hochberg false discovery rate adjustment applied
443 for multiple testing corrections.⁴⁷

445 Bacterial culture steroid reductase assay

446 A complete list of strains used in this study is provided in **Supplementary Table 2**.
447 Strains were incubated under anaerobic conditions (85% N₂, 10% CO₂, 5% H₂) at 37 °C in an
448 anaerobic chamber (Coy Laboratory). Liquid brain-heart infusion (BHI) broth supplemented with
449 100 µM steroids from 10 mM stocks in methanol was used for growth. Cultures were grown
450 anaerobically with a 1% (v/v) inoculum from a pre-culture and supplemented with steroids after
451 4 hours of incubation during the exponential growth phase. Bacterial cultures were extracted by
452 the addition of 9 volumes of methanol supplemented with 0.5 µM methylprednisolone as an
453 internal standard for LC-MS analysis.

454 LC-MS-Q-TOF analysis of steroids

455 Extracted samples were vortexed and centrifuged twice at 21,000 × g for 15 minutes,
456 with the supernatant transferred to new tubes after each centrifugation step. The methanol
457 fraction was filtered through 0.2 µm nylon membrane filters prior to LC-MS analysis. Samples
458 were analyzed using an Agilent 6540 UHD Q-TOF mass spectrometer coupled to an Agilent
459 1200 Infinity LC system. Separation was performed on a XBridge C18 column (2.1x100mm, 3.5
460 µm particle size) using 0.1% aqueous formic acid and acetonitrile with 0.1% formic acid as
461 mobile phases. The separation gradient ranged from 20% to 100% acetonitrile over 4 minutes at
462 50 °C with a flow rate of 0.5 mL/min. Mass spectra were acquired in negative ion mode for
463 glucocorticoids ([M+FA-H]⁻) or positive ion mode for all other steroids ([M+H]⁺), with an ion spray
464 voltage of 3500 V and a nozzle voltage of 2000 V. The source temperature was set to 300 °C,
465 and the gas flow rate was 8 L/min. Data were processed and visualized using MassHunter
466 software version 10.

467 Molecular biology

468 Gene transformations were performed by Gibson assembly using 2x NEBuilder® HiFi
469 DNA Assembly Master Mix (New England Biolabs, NEB, E2621X). Primers were designed using
470 SnapGene (see **Supplementary Table 7**), incorporating 20 bp flanking regions complementary
471 to a linearized expression vector (pMCSG53) and the gene of interest from the HCS.1 genome.
472 PCR, cloning, and transformation were performed according to the protocols provided on the
473 NEB website. The Gibson assembly reaction was incubated at 50 °C for 1 hour and then
474 transformed into *E. coli* XL1-Blue competent cells according to the manufacturer's protocol.
475 Transformed cells were plated on Luria-Bertani (LB) agar plates containing 100 µg/mL
476 carbenicillin, and successful transformations were confirmed using sequencing primers specific
477 for the backbone vector (see **Supplementary Table 7**). Positive colonies were validated and
478 sequenced by the University of Chicago Genomics Facility. The final constructs were then
479 transformed into chemically competent *E. coli* Rosetta™ (DE3) competent cells (Novagen)
480 according to NEB protocols. Transformed cells were plated on LB agar plates supplemented
481 with 100 µg/mL carbenicillin.

482 Protein production in *E. coli*

483 Protein production in *E. coli* Rosetta cells was performed under aerobic conditions for all
484 short-chain dehydrogenases (SDRs) and under anaerobic conditions for OsrA and OsrB.
485 Cultures were grown in either 2x YT medium (20 g/L tryptone, 10 g/L yeast extract, and 5 g/L
486 NaCl) or TB medium (12 g/L tryptone, 24 g/L yeast extract, 4 mL/L glycerol, 9.4 g/L K₂HPO₄,
487 and 2.2 g/L KH₂PO₄) supplemented with 0.5% (w/v) glucose and 1 mM ferric ammonium citrate,
488 respectively.

489 Induction of protein expression was initiated during the exponential phase when optical
490 densities (OD₆₀₀) reached 0.4-0.6 by the addition of 1 mM isopropyl β-D-1-
491 thiogalactopyranoside (IPTG). Cultures were incubated for 3-5 hours at 37 °C with shaking at
492 200 rpm. Cells were harvested by centrifugation at 4500 × g for 20 minutes. Cell pellets were

496 then frozen at -80 °C for storage prior to subsequent experimental use. Protein production was
497 confirmed by SDS-PAGE analysis.

498

499 Purification of heterologous produced proteins

500 *Cell Lysis and Protein Purification.* Frozen cell pellets were supplemented with 0.1 mg/mL
501 DNase and lysed either aerobically (for SDRs) or anaerobically (for OsrA and OsrB) using a
502 Thermo Spectronic French pressure cell at 1,100 PSI. The crude cell extract was centrifuged at
503 75,600 x g for 30 minutes, followed by filtration through a 0.2 µm nylon membrane (Fisher
504 Scientific) before being applied to a purification system.

505

506 *Aerobic purification of SDRs.* The filtered extract was applied to an ÄKTA pure system (Cytiva)
507 using a 1 mL Strep-Tactin®XT 4Flow® column (Iba Lifesciences). The column was equilibrated
508 with 10 volumes of equilibration buffer (100 mM Tris/HCl, pH 8.0, 150 mM NaCl) at 1 mL/min
509 and 4°C. Proteins were loaded via a 5 mL loop, followed by washing of non-specifically bound
510 proteins. Elution was performed with 5 mL elution buffer (100 mM Tris/HCl, pH 8.0, 150 mM
511 NaCl, and 50 mM biotin). Eluted proteins were collected in 1 mL fractions and were
512 concentrated using Pierce™ Protein concentrators (10 kDa), desalted, and either used directly
513 or transferred to storage buffer (50 mM Tris/HCl, pH 7.5, 10% (w/v) glycerol, and 50 mM NaCl)
514 using PD-10 desalting columns (Cytiva) before storage at -80 °C.

515

516 *Anaerobic purification of OsrB.* Anaerobic purification was performed in an anaerobic chamber.
517 A Strep-Tactin®XT 4Flow® gravity column (Iba Lifesciences) was used with a WET FRED
518 system (Iba Lifesciences) to maintain a constant flow rate of ~1 mL/min, adjusted using a lab
519 jack stand (LABALPHA). The column was equilibrated with anaerobic equilibration buffer (100
520 mM Tris/HCl, pH 8.0, 150 mM NaCl) and elution was performed with anaerobic elution buffer
521 (100 mM Tris/HCl, pH 8.0, 150 mM NaCl, and 50 mM biotin). Eluted proteins were collected in 1
522 mL tubes, concentrated and desalted using Pierce™ Protein Concentrators PES, 10K MWCO,
523 0.5 mL, at 10,000 x g in a microcentrifuge. Proteins were either used directly for enzymatic
524 assays or transferred to anaerobic storage buffer (50 mM Tris/HCl, pH 7.5, 10% (w/v) glycerol,
525 and 50 mM NaCl) and frozen at -80 °C.

526

527 Whole-cell assays of heterologous enzymes

528 The activity of heterologously expressed proteins was assessed under either aerobic
529 conditions (for SDRs) or anaerobic conditions (for OsrA and OsrB). *E. coli* Rosetta cells were
530 grown in media as described above, supplemented with 100 µM steroids (prepared from 10 mM
531 stock solutions in methanol) using a 1% (v/v) inoculum. Protein production was induced with 1
532 mM IPTG at an OD of 0.4-0.7 and cultures were incubated overnight at 37 °C without shaking.
533 Reactions were quenched by the addition of 9 volumes of methanol containing 0.5 µM
534 methylprednisolone as internal standard (IS). LC-MS samples were prepared as described
535 previously.

536

537 Enzymatic assays with purified SDRs

538 The kinetic properties of purified SDRs were determined using reaction mixtures in 96-
539 well plates with a total volume of 100 µL. The reaction mixture contained 25 mM Tris/HCl (pH
540 7.0), 1 mM NADPH, 10 µM to 1 mM steroids (diluted in 20 mM hydroxypropyl-β-cyclodextrin),
541 and 0.01 to 0.5 mg/mL protein, depending on the enzyme activity. Enzyme activity was
542 monitored by measuring the reduction of NADPH at 340 nm using a plate reader (BioTek,
543 Cytation 5) at 37°C. A NADPH standard curve was analyzed under identical conditions with an
544 extinction coefficient of 1398 M⁻¹ for quantitation.

545

546 Enzymatic assays with purified OsrA and OsrB

547 The substrate preferences of OsrA and OsrB were analyzed under anaerobic conditions
548 using a 100 μ L reaction mixture containing 50 mM Tris/HCl (pH 7.0), 200 μ M methyl viologen,
549 0.5 mM steroids (from 10x stock solutions in methanol), and 50 μ g/mL protein. Enzyme activity
550 was monitored by measuring electron donor reduction at 605 nm using a plate reader (BioTek,
551 Epoch 2) at 37°C. Quantification was performed using an electron donor standard curve
552 generated under the same conditions with an extinction coefficient of 1689 M⁻¹ for quantitation.
553

554 Phylogenetic tree construction

555 Genome metadata were retrieved from a local UHGG database and used to map
556 genome IDs to species names. A comparative analysis was performed using BLASTp
557 (version 2.15.0+) to search for homologs of the target sequence against the UHGP-100
558 database, limiting results to the top 20000 hits. The BLASTp output was processed to map
559 genome IDs to species names and format the sequences in FASTA format, removing
560 duplicates to ensure data quality. Additional sequences were appended to the data set as
561 needed. Sequence alignment was performed using Clustal Omega (version 1.2.2)⁴⁸ with
562 output formatted as FASTA. Header sanitization was performed to remove special characters,
563 and duplicate sequences were filtered out using custom Python scripts to maintain alignment
564 integrity. Phylogenetic analysis was performed using IQ-TREE (version 2.3.6)⁴⁹ with
565 automatic model selection to determine the best-fitting substitution model based on the data.
566 The reliability of the phylogenetic trees was assessed using 1,000 ultrafast bootstrap
567 replicates to assess branch support. The final phylogenetic trees were visualized and
568 interpreted using the Interactive Tree of Life (iTOL)⁵⁰ to explore the evolutionary relationships
569 among the identified protein sequences.
570

571 Metagenomics

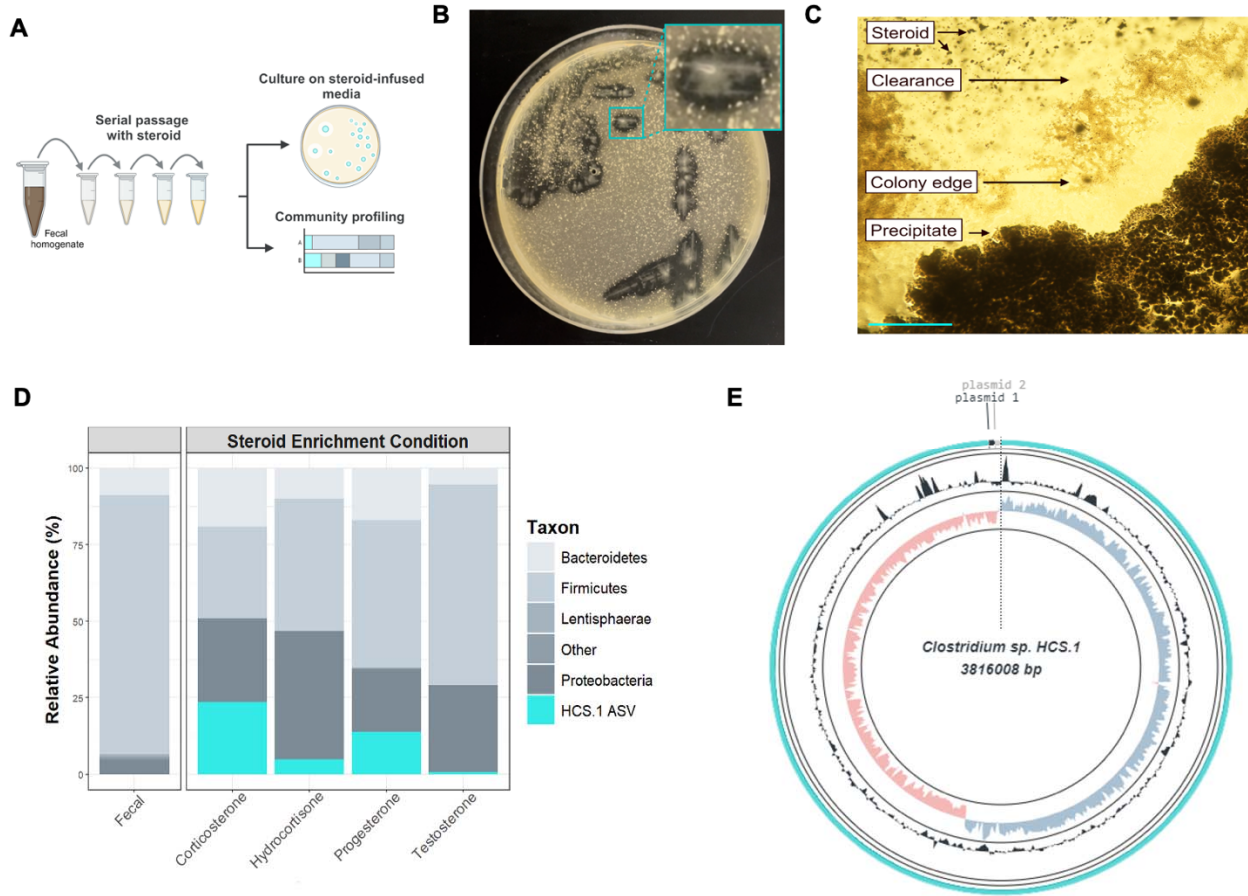
572 To identify relevant sequences of OsrA or OsrB, a BLAST search was first conducted
573 against the UHGP-100 database, applying a 49% similarity threshold based on experimental
574 evidence indicating that this threshold effectively identifies relevant homologs while minimizing
575 false positives. For OsrB, the identified protein sequences were used to construct a
576 phylogenetic tree using Clustal Omega for alignment and IQ-TREE with the "mtest" model
577 selection and 1,000 bootstrap replicates as described above. Based on the initial analysis, 25
578 sequences that were not phylogenetically related to OsrB were manually excluded. This
579 curation step ensured that only sequences relevant to the target enzymes were retained for
580 downstream analysis.

581 After phylogenetic filtering, genome information was traced back using the UHGP protein
582 IDs. The corresponding genomes were downloaded from the Unified Human Gastrointestinal
583 Genome (UHGG) database using FTP links provided in the metadata file. The genomes were
584 then used for further analysis, where each protein sequence was screened against the
585 respective genome using tblastn with a stringent e-value threshold of 1e⁻²⁰⁰ to ensure high
586 specificity. The best nucleotide sequence was selected for each protein based on coverage and
587 bit score and subsequently compiled into a combined FASTA file.

588 Metagenomic samples were downloaded from the Sequence Read Archive (SRA). Reads were
589 quality trimmed to remove adapter sequences using TrimGalore with default settings,⁵¹ and
590 potential human contamination was removed by mapping the reads to the human reference
591 genome (T2T-CHM13v2.0) using Bowtie2 (version 2.5.3) and removing the mapped reads with
592 Samtools (version 1.61.1).^{52,53} Samples were then mapped to the gene reference datasets for
593 *osrA* and *osrB* using Bowtie2 (version 2.5.3), and copies per million (CPM values) were
594 calculated for each gene in each sample. Samples with total read counts below 1,000,000 were
595 excluded.

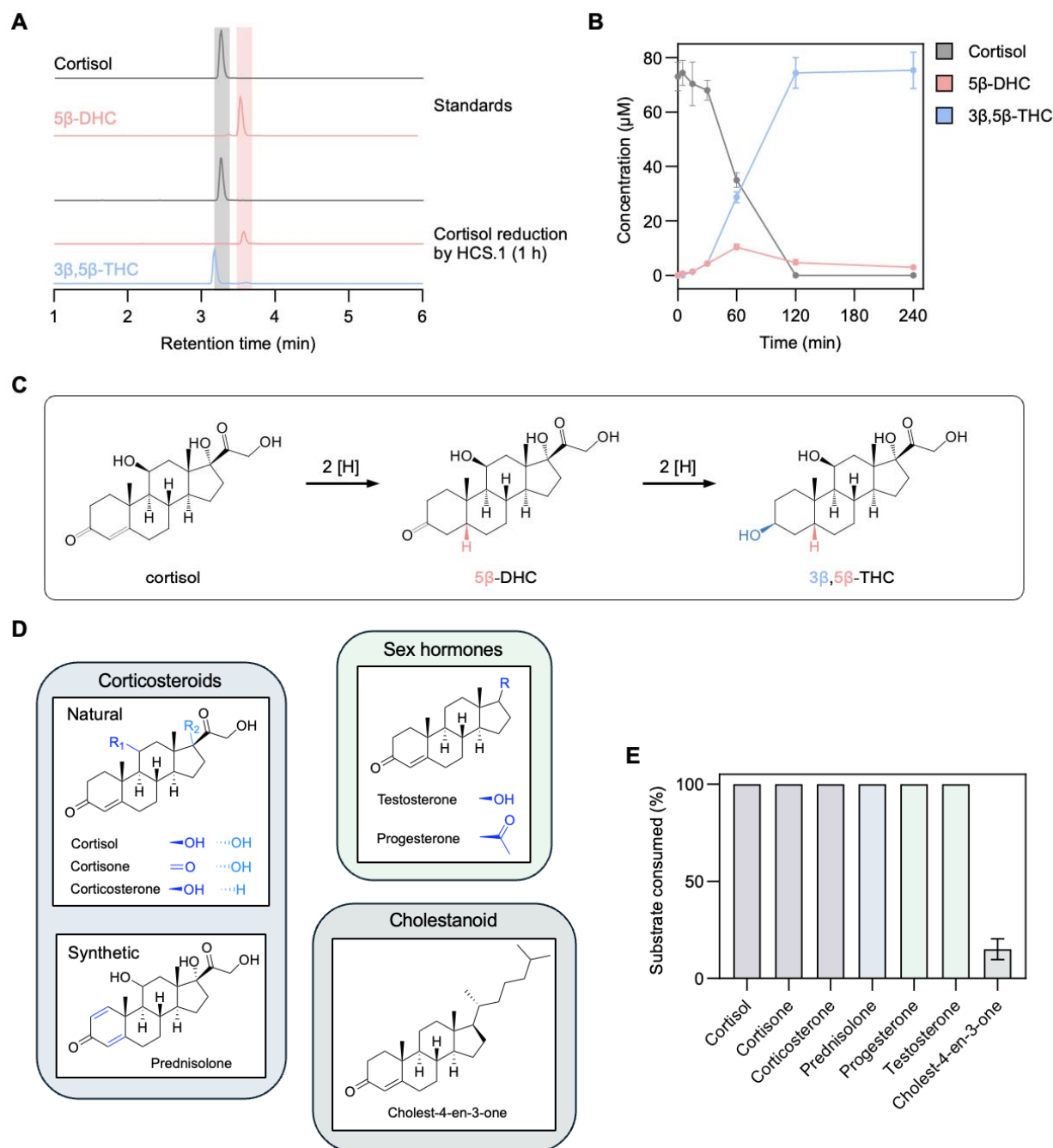
596 Metagenomic data were filtered to ensure quality for statistical analyses. Zero values
597 were replaced with 1e⁻⁶ for statistical assessment. A 99th percentile filter was applied to CPM

598 values for each gene (*osrA* and *osrB*) to remove extreme outliers. Normality was assessed
599 using the Shapiro-Wilk test; if both groups were normal ($p > 0.05$), a two-sided Welch's t-test
600 was used to determine if there was any significant difference between the groups, regardless of
601 direction. If normality was not met, a two-sided Mann-Whitney U test was applied. This
602 conservative approach ensured that differences were detected without assuming the direction of
603 the effect, providing flexibility in hypothesis testing. Analyses were performed using Python with
604 Scipy, Pandas, and Seaborn libraries.



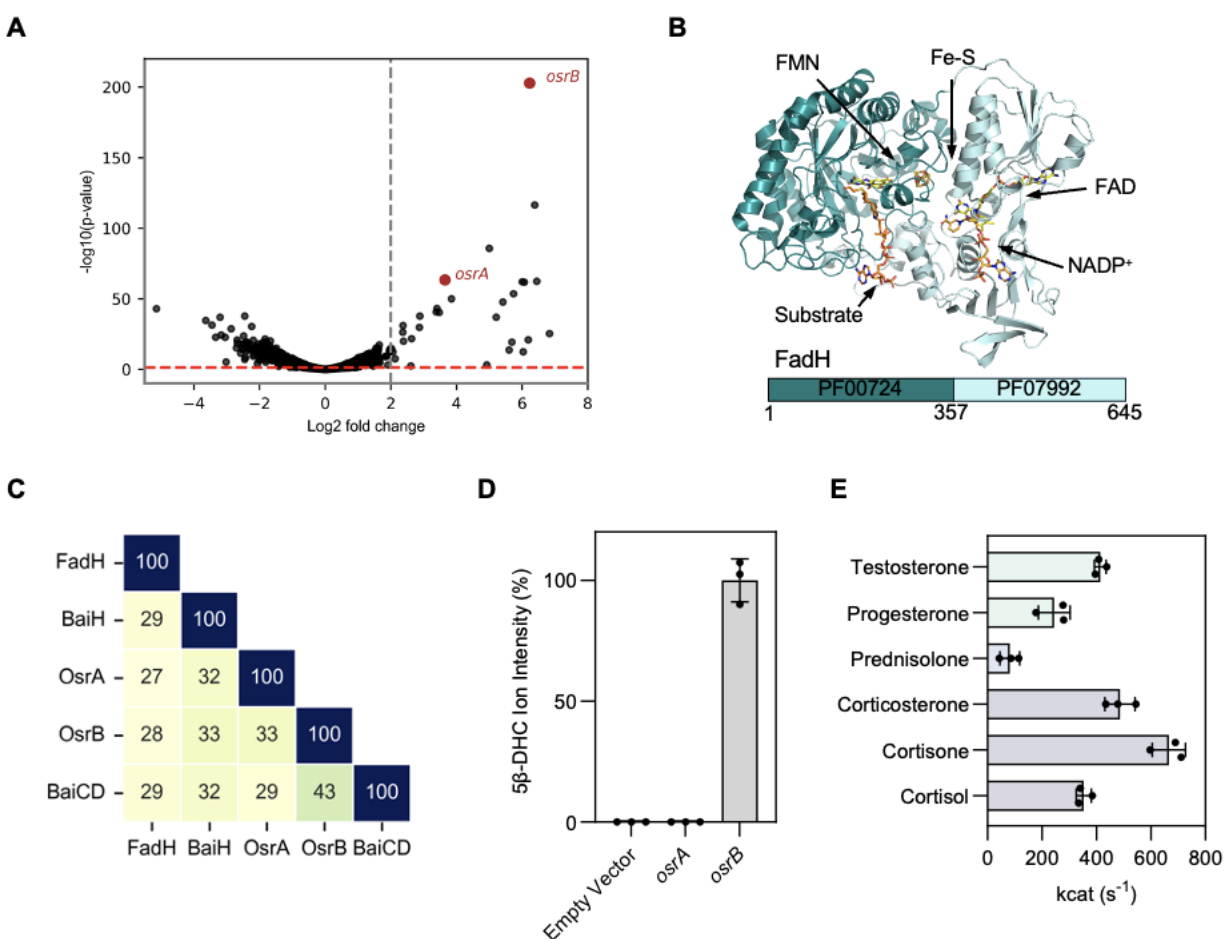
605
606
607
608
609
610
611

Figure 1. *Clostridium steroidoreducens* is a novel steroid-enriched species. (A) Schematic overview of steroid enrichment and strain isolation experiments. (B) HCS.1 strain colonies on cortisol-infused media. (C) HCS.1 strain colonies on progesterone-infused media. Scale bar, 200 µm. (D) Microbial community profile of the final steroid hormone enrichment passage based on 16S rRNA amplicon sequencing. (E) Circular representation of the HCS.1 genome.

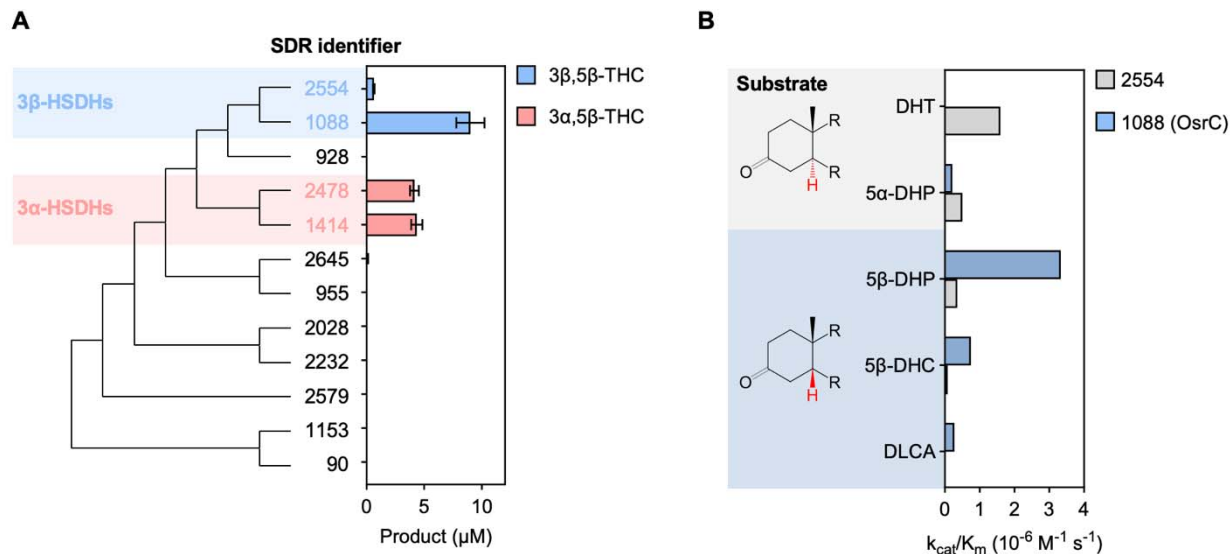


612
613
614
615
616
617
618
619

Figure 2. *C. steroidoreducens* HCS.1 possesses promiscuous 3-oxo- Δ^4 -beta steroid hormone reductase activity. (A) Products formed from *C. steroidoreducens* HCS.1 incubation with cortisol. (B) Time-course analysis of cortisol metabolism by *C. steroidoreducens* HCS.1. (C) Proposed pathway for cortisol reduction by *C. steroidoreducens* HCS.1. DHC and THC stand for dihydrocortisol and tetrahydrocortisol, respectively. (D) Steroid substrates tested for *C. steroidoreducens* HCS.1. (E) Measured *C. steroidoreducens* HCS.1 steroid substrate consumption.

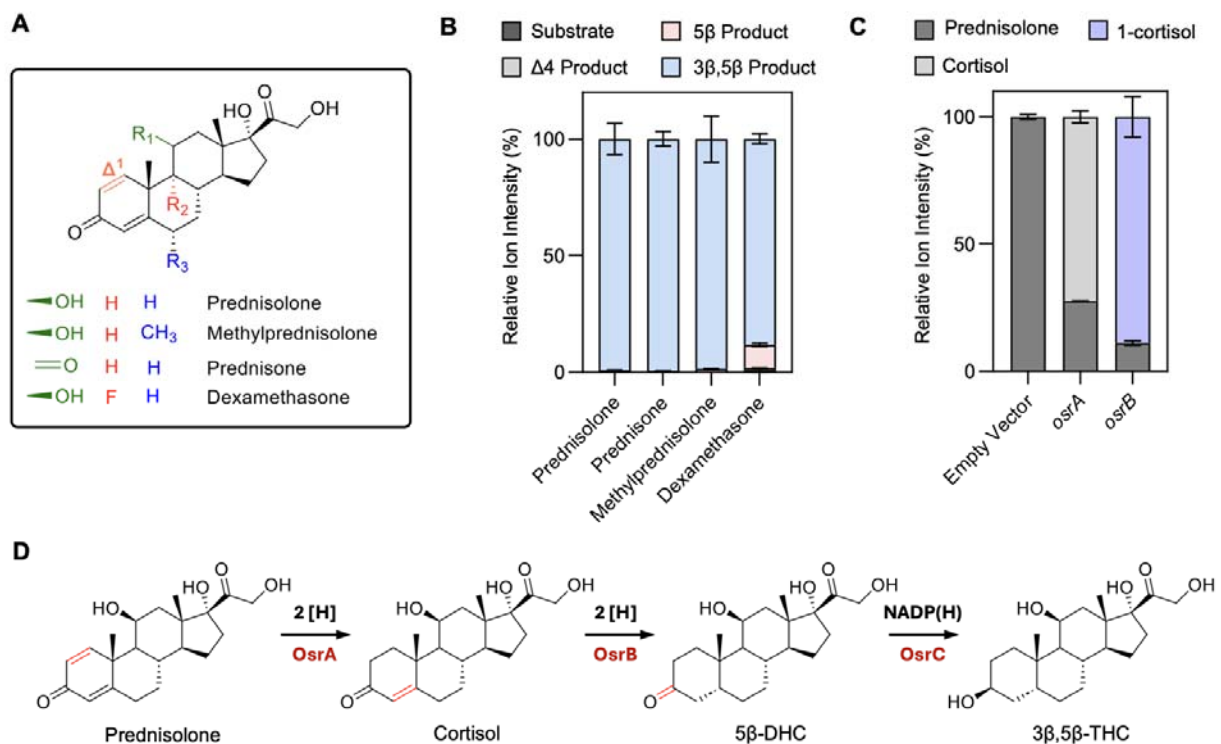


620
 621 **Figure 3. OsrB is a 3-oxo- Δ^4 -steroid hormone reductase.** (A) Gene expression of *C. steroidoreducens*
 622 HCS.1 in the presence versus absence of cortisol. Gray and red dashed lines indicate genes with
 623 statistical significance and >2-fold induction in response to cortisol, respectively. (B) Crystal structure of
 624 Fe-S flavoenzyme 2,4-dienoyl-CoA reductase (FadH) bound to ligands (PDB code: 1PS9). (C) Percent
 625 sequence identity of OsrA and OsrB to Fe-S flavoenzymes FadH and bile acid reductases BaiH and
 626 BaiCD. (D) Conversion of cortisol to 5 β -dihydrocortisol (DHC) by *E. coli* expressing *osrA* or *osrB* versus
 627 an empty vector control. (E) Rate of reduction of indicated steroid hormones by purified OsrB.



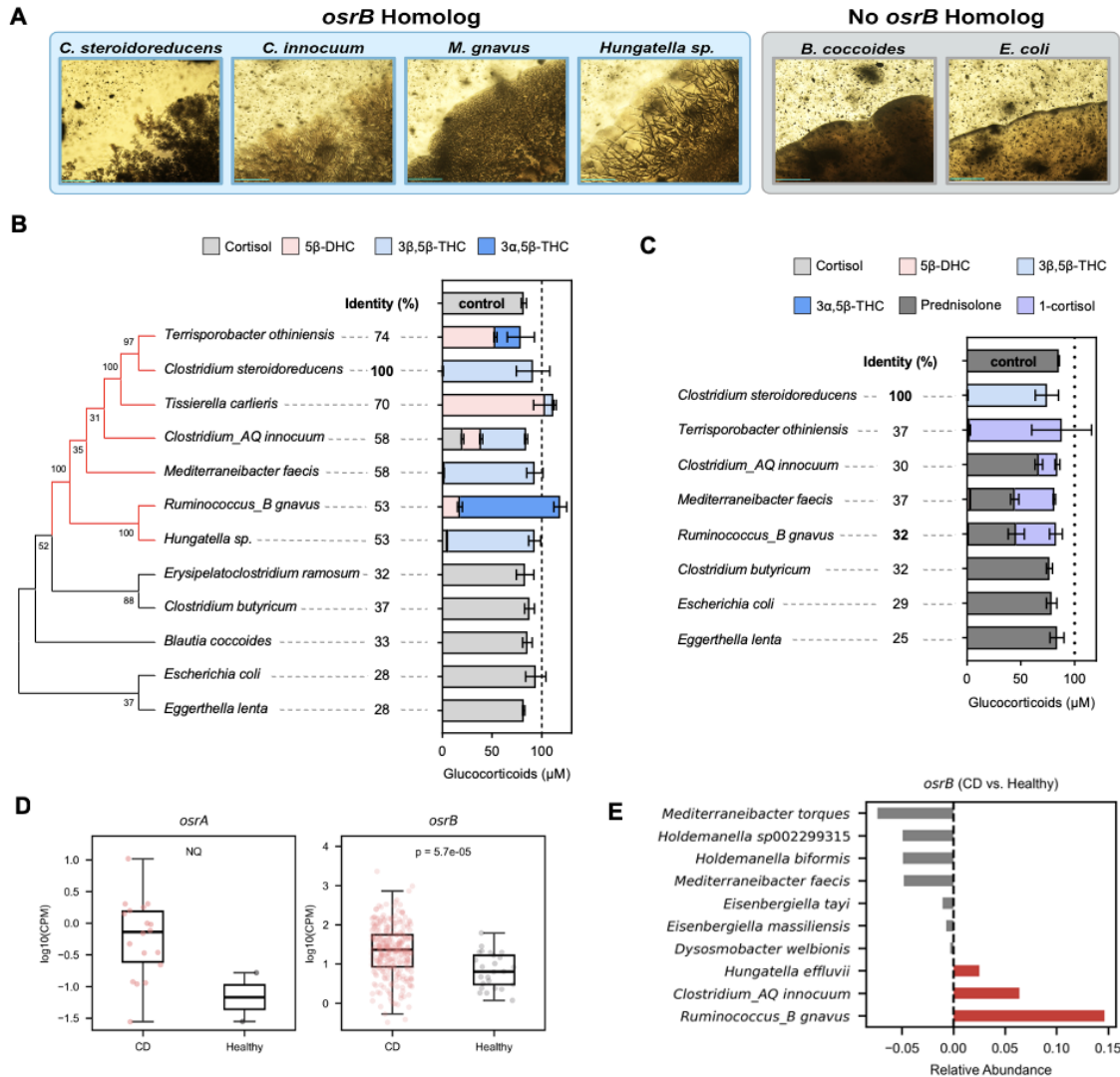
628
629
630
631
632
633
634
635
636

Figure 4. OsrC is a 3-oxo-5β-steroid hormone oxidoreductase. (A) Phylogenetic analysis of *C. steroidoreducens* HCS.1 SDR domain-containing protein sequences. Product formed from 5β-dihydrocortisol by *E. coli* strains overexpressing SDR domain-containing proteins are shown with their respective gene identifiers. THC stand for tetrahydrocortisol. (B) Kinetic parameters of reduction of indicated steroid hormones by purified SDR domain-containing proteins. Abbreviations stand for dihydrotestosterone (DHT), dihydroprogesterone (DHP), dihydrocortisol (DHC), and dehydrolithocholic acid (DLCA).



637
638
639
640
641
642
643
644

Figure 5. OsrA is a 3-oxo- Δ^1 -reductase essential for complete reduction of synthetic corticosteroids. (A) Structure of synthetic corticosteroids used in assays. (B) Products formed from synthetic corticosteroids following incubation with *C. steroidoreducens* HCS.1 cells. (C) Percent prednisolone conversion to cortisol following incubation of *E. coli* cells with *osrA*- and *osrB*-expressing plasmids or an empty vector control. (D) *C. steroidoreducens* HCS.1 steroid reduction pathway identified in this study.



645
646 **Figure 6. Steroid reductase activities are widespread in gut bacteria and elevated in active Crohn's**
647 **disease.** (A) Representative images of gut bacteria grown on progesterone-infused media, showing
648 steroid clearance/precipitate accumulation-positive (blue background) and -negative (gray background)
649 colonies. Scale bar, 200 μm. (B) Corticosteroids produced by gut bacterial isolates after incubation with
650 cortisol. The protein with the highest sequence identity to *OsrB* encoded by each genome was used to
651 generate the tree. (C) Corticosteroids produced by gut bacterial isolates after incubation with
652 prednisolone. Identity refers to the sequence identity of the protein with the highest sequence identity to
653 *OsrA* encoded by each genome. (D) reads mapping to *osrA* and *osrB* homologs in metagenomes from
654 healthy and Crohn's disease (CD) patients. Only metagenomes with at least one read mapping to a gene
655 are included in the analysis. NQ refers to the not quantified statistical difference, due to the low number of
656 healthy metagenomes with reads mapping to *osrA*. CPM refers to copies per million. (E) Difference in
657 *osrB* homolog abundance for taxa showing the greatest changes in relative abundance between healthy
658 and CD metagenomes.

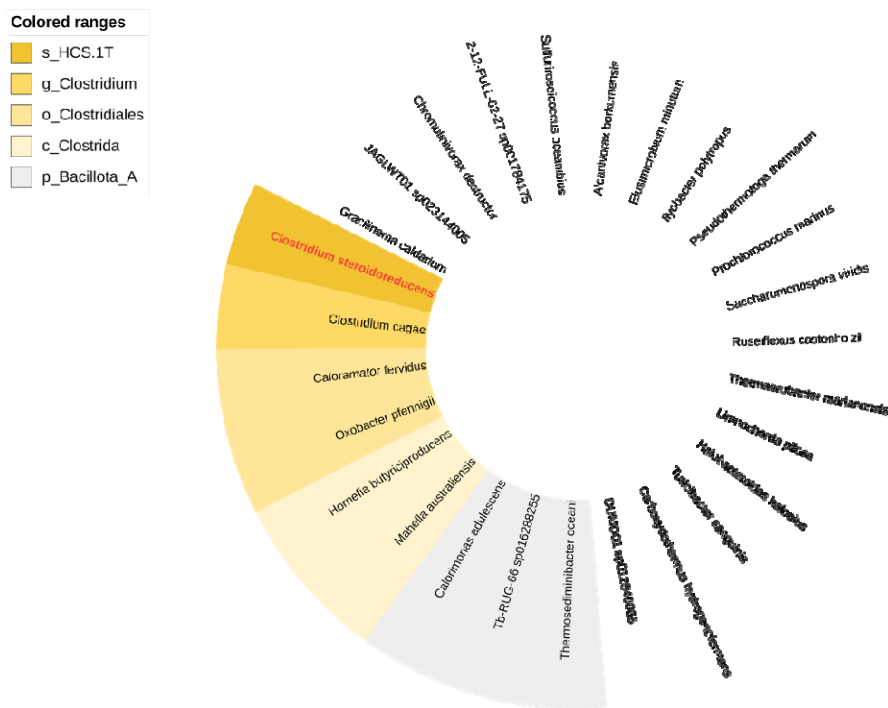
659 **REFERENCES**

- 660 1. Nussey, S. & Whitehead, S. The adrenal gland. in *Endocrinology: An Integrated Approach* (BIOS
661 Scientific Publishers, 2001).
- 662 2. Nussey, S. & Whitehead, S. The gonad. in *Endocrinology: An Integrated Approach* (BIOS
663 Scientific Publishers, 2001).
- 664 3. Buffie, C. G. et al. Precision microbiome reconstitution restores bile acid mediated resistance to
665 *Clostridium difficile*. *Nature* 517, 205–208 (2015).
- 666 4. Paik, D. et al. Human gut bacteria produce TH17-modulating bile acid metabolites. *Nature* 603,
667 907–912 (2022).
- 668 5. Campbell, C. et al. Bacterial metabolism of bile acids promotes generation of peripheral
669 regulatory T cells. *Nature* 581, 475–479 (2020).
- 670 6. Adlercreutz, H., Martin, F., Järvenpää, P. & Fotsis, T. Steroid absorption and enterohepatic
671 recycling. *Contraception* 20, 201–223 (1979).
- 672 7. Decker, H. A. et al. Metabolism of 4-C 14-cortisol in man: body distribution and rates of
673 conjugation. *J. Clin. Endocrinol. Metab.* 16, 1137–1150 (1956).
- 674 8. Peterson, R. E., Wyngaarden, J. B., Guerra, S. L., Brodie, B. B. & Bunim, J. J. THE
675 PHYSIOLOGICAL DISPOSITION AND METABOLIC FATE OF HYDROCORTISONE IN MAN. *J.*
676 *Clin. Invest.* 34, 1779–1794 (1955).
- 677 9. Sandberg, A. A. & Slaunwhite, W. R. Metabolism of 4-C14-testosterone in human subjects. I.
678 Distribution in bile, blood, feces and urine. *J. Clin. Invest.* 35, 1331–1339 (1956).
- 679 10. Adlercreutz, H. & Martin, F. Biliary excretion and intestinal metabolism of progesterone and
680 estrogens in man. *J. Steroid Biochem.* 13, 231–244 (1980).
- 681 11. Migeon, C. J., Paul, A. C., Samuels, L. T. & Sandberg, A. A. Metabolism of 4-C14-corticosterone
682 in man. *J. Clin. Endocrinol. Metab.* 16, 1291–1298 (1956).
- 683 12. Möstl, E. & Palme, R. Hormones as indicators of stress. *Domest. Anim. Endocrinol.* 23, 67–74
684 (2002).
- 685 13. Palme, R., Rettenbacher, S., Touma, C., El-Bahr, S. M. & Möstl, E. Stress hormones in mammals
686 and birds: comparative aspects regarding metabolism, excretion, and noninvasive measurement
687 in fecal samples. *Ann. N. Y. Acad. Sci.* 1040, 162–171 (2005).
- 688 14. Nabarro, J. D., Moxham, A., Walker, G. & Slater, J. D. Rectal hydrocortisone. *Br. Med. J.* 2, 272–
689 274 (1957).
- 690 15. Wade, A. P., Slater, J. D., Kellie, A. E. & Holliday, M. E. Urinary excretion of 17-ketosteroids
691 following rectal infusion of cortisol. *J. Clin. Endocrinol. Metab.* 19, 444–453 (1959).
- 692 16. Martin, F., Peltonen, J., Laatikainen, T., Pulkkinen, M. & Adlercreutz, H. Excretion of progesterone
693 metabolites and estriol in faeces from pregnant women during ampicillin administration. *J. Steroid*
694 *Biochem.* 6, 1339–1346 (1975).
- 695 17. Ly, L. K. et al. Bacterial steroid-17,20-desmolase is a taxonomically rare enzymatic pathway that
696 converts prednisone to 1,4-androstenediene-3,11,17-trione, a metabolite that causes proliferation
697 of prostate cancer cells. *J. Steroid. Biochem. Mol. Biol.* 199, 105567 (2020).
- 698 18. Zimmermann, M., Zimmermann-Kogadeeva, M., Wegmann, R. & Goodman, A. L. Mapping
699 human microbiome drug metabolism by gut bacteria and their genes. *Nature* 570, 462–467
700 (2019).
- 701 19. Latif, S. A., Sheff, M. F., Ribeiro, C. E. & Morris, D. J. Selective inhibition of sheep kidney 11 β -
702 hydroxysteroid dehydrogenase isoform 2 activity by 5 α -reduced (but not 5 β) derivatives of
703 adrenocorticosteroids. *Steroids* 62, 230–237 (1997).
- 704 20. Honour, J. W., Borriello, S. P., Ganten, U. & Honour, P. Antibiotics attenuate experimental
705 hypertension in rats. *J. Endocrinol.* 105, 347–350 (1985).
- 706 21. N, P. et al. Commensal bacteria promote endocrine resistance in prostate cancer through
707 androgen biosynthesis. *Science* 374, (2021).

- 708 22. Terrisse, S., Zitvogel, L. & Kroemer, G. Effects of the intestinal microbiota on prostate cancer
709 treatment by androgen deprivation therapy. *Microb. Cell Graz Austria* 9, 202–206 (2022).
- 710 23. Stokes, N. A. & Hylemon, P. B. Characterization of delta 4-3-ketosteroid-5 beta-reductase and 3
711 beta-hydroxysteroid dehydrogenase in cell extracts of *Clostridium innocuum*. *Biochim. Biophys.*
712 *Acta* **836**, 255–261 (1985).
- 713 24. Penning, T. M. & Covey, D. F. 5 β -Dihydrosteroids: Formation and Properties. *Int. J. Mol. Sci.* **25**,
714 8857 (2024).
- 715 25. Parks, D. H. et al. A standardized bacterial taxonomy based on genome phylogeny substantially
716 revises the tree of life. *Nat. Biotechnol.* 36, 996–1004 (2018).
- 717 26. McCurry, M. D. et al. Gut bacteria convert glucocorticoids into progestins in the presence of
718 hydrogen gas. *Cell* 187, 2952-2968.e13 (2024).
- 719 27. Devendran, S., Mythen, S. M. & Ridlon, J. M. The desA and desB genes from *Clostridium*
720 *scindens* ATCC 35704 encode steroid-17,20-desmolase. *J. Lipid Res.* **59**, 1005–1014 (2018).
- 721 28. Maini Rekdal, V. et al. A widely distributed metalloenzyme class enables gut microbial metabolism
722 of host- and diet-derived catechols. *eLife* 9, e50845 (2020).
- 723 29. Hubbard, P. A., Liang, X., Schulz, H. & Kim, J.-J. P. The crystal structure and reaction mechanism
724 of *Escherichia coli* 2,4-dienoyl-CoA reductase. *J. Biol. Chem.* 278, 37553–37560 (2003).
- 725 30. Little, A. S. et al. Dietary- and host-derived metabolites are used by diverse gut bacteria for
726 anaerobic respiration. *Nat. Microbiol.* 9, 55–69 (2024).
- 727 31. Funabashi, M. et al. A metabolic pathway for bile acid dehydroxylation by the gut microbiome.
728 *Nature* 582, 566–570 (2020).
- 729 32. Kang, D.-J., Ridlon, J. M., Moore, D. R., Barnes, S. & Hylemon, P. B. *Clostridium scindens* baiCD
730 and baiH genes encode stereo-specific 7 α /7 β -hydroxy-3-oxo- Δ^4 -cholenoic acid
731 oxidoreductases. *Biochim. Biophys. Acta* 1781, 16–25 (2008).
- 732 32. Edenharder, R. & Schneider, J. 12 beta-dehydrogenation of bile acids by *Clostridium*
733 *paraputrificum*, *C. tertium*, and *C. difficile* and epimerization at carbon-12 of deoxycholic acid by
734 cocultivation with 12 alpha-dehydrogenating *Eubacterium lentum*. *Appl. Environ. Microbiol.* **49**,
735 964–968 (1985).
- 736 33. Doden, H. L. & Ridlon, J. M. Microbial Hydroxysteroid Dehydrogenases: From Alpha to Omega.
737 *Microorganisms* 9, 469 (2021).
- 738 34. Doden, H. et al. Metabolism of Oxo-Bile Acids and Characterization of Recombinant 12 α -
739 Hydroxysteroid Dehydrogenases from Bile Acid 7 α -Dehydroxylating Human Gut Bacteria. *Appl.*
740 *Environ. Microbiol.* **84**, e00235-18 (2018).
- 741 35. Ardizzone, S. & Bianchi Porro, G. Comparative tolerability of therapies for ulcerative colitis. *Drug*
742 *Saf.* 25, 561–582 (2002).
- 743 36. Yang, R. & Yu, Y. Glucocorticoids are double-edged sword in the treatment of COVID-19 and
744 cancers. *Int. J. Biol. Sci.* 17, 1530–1537 (2021).
- 745 37. Almeida, A. et al. A unified catalog of 204,938 reference genomes from the human gut
746 microbiome. *Nat. Biotechnol.* 39, 105–114 (2021).
- 747 38. Lewis, J. D. et al. Inflammation, Antibiotics, and Diet as Environmental Stressors of the Gut
748 Microbiome in Pediatric Crohn’s Disease. *Cell Host Microbe* 18, 489–500 (2015).
- 749 39. Ha, C. W. Y. et al. Translocation of Viable Gut Microbiota to Mesenteric Adipose Drives Formation
750 of Creeping Fat in Humans. *Cell* 183, 666-683.e17 (2020).
- 751 40. Hall, A. B. et al. A novel *Ruminococcus gnavus* clade enriched in inflammatory bowel disease
752 patients. *Genome Med.* 9, 103 (2017).
- 753 41. Lloyd-Price, J. et al. Multi-omics of the gut microbial ecosystem in inflammatory bowel diseases.
754 *Nature* **569**, 655–662 (2019).
- 755 42. Arp, G. et al. Gut Bacteria Encode Reductases that Biotransform Steroid Hormones. *bioRxiv*
756 2024.10.04.616736 (2024) doi:10.1101/2024.10.04.616736.

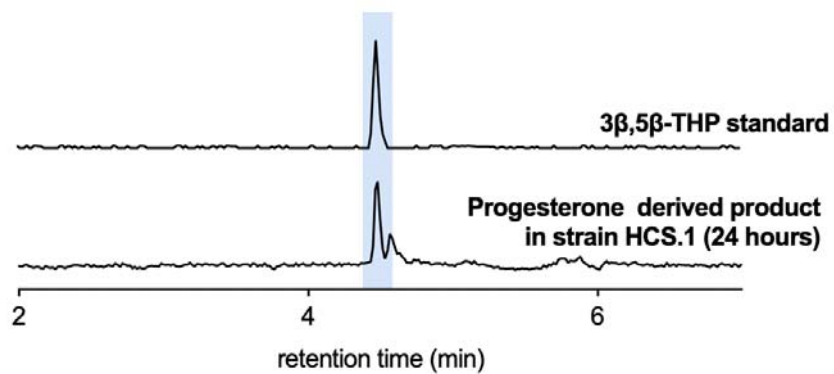
- 757 43. Wick, R. R., Judd, L. M., Gorrie, C. L. & Holt, K. E. Unicycler: Resolving bacterial genome
758 assemblies from short and long sequencing reads. *PLoS Comput. Biol.* 13, e1005595 (2017).
- 759 44. Wick, R. R., Judd, L. M., Gorrie, C. L. & Holt, K. E. Completing bacterial genome assemblies with
760 multiplex MinION sequencing. *Microb. Genomics* 3, e000132 (2017).
- 761 45. Chaumeil, P.-A., Mussig, A. J., Hugenholtz, P. & Parks, D. H. GTDB-Tk: a toolkit to classify
762 genomes with the Genome Taxonomy Database. *Bioinformatics* 36, 1925–1927 (2019).
- 763 46. O, S. *et al.* Bakta: rapid and standardized annotation of bacterial genomes via alignment-free
764 sequence identification. *Microb. Genomics* 7, (2021).
- 765 47. Mi, L., W, H. & S, A. Moderated estimation of fold change and dispersion for RNA-seq data with
766 DESeq2. *Genome Biol.* 15, (2014).
- 767 48. Sievers, F. *et al.* Fast, scalable generation of high-quality protein multiple sequence alignments
768 using Clustal Omega. *Mol. Syst. Biol.* 7, 539 (2011).
- 769 49. Nguyen, L.-T., Schmidt, H. A., von Haeseler, A. & Minh, B. Q. IQ-TREE: a fast and effective
770 stochastic algorithm for estimating maximum-likelihood phylogenies. *Mol. Biol. Evol.* 32, 268–274
771 (2015).
- 772 50. Letunic, I. & Bork, P. Interactive Tree Of Life (iTOL): an online tool for phylogenetic tree display
773 and annotation. *Bioinformatics* 23, 127–128 (2007).
- 774 51. Krueger, F. *et al.* FelixKrueger/TrimGalore: v0.6.10. *Zenodo* doi: [10.5281/zenodo.7598955](https://doi.org/10.5281/zenodo.7598955)
775 (2023).
- 776 52. Langmead, B. & Salzberg, S. L. Fast gapped-read alignment with Bowtie 2. *Nat. Methods* 9, 357–
777 359 (2012).
- 778 53. H, L. *et al.* The Sequence Alignment/Map format and SAMtools. *Bioinforma. Oxf. Engl.* 25,
779 (2009).

780



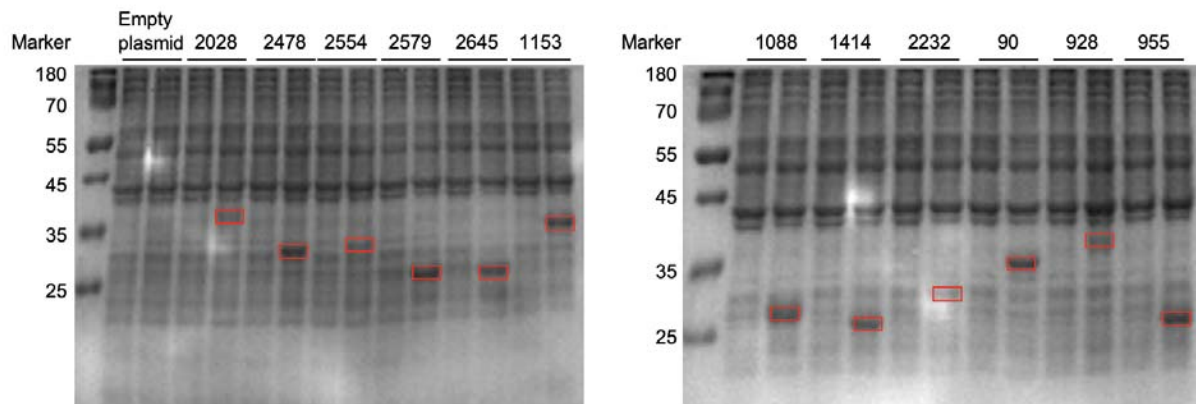
781
782
783
784

Extended Data Figure 1. Phylogenetic analysis supporting assignment of HCS.1 within the *Clostridium* genus. Tree generated from alignment of conserved marker genes.



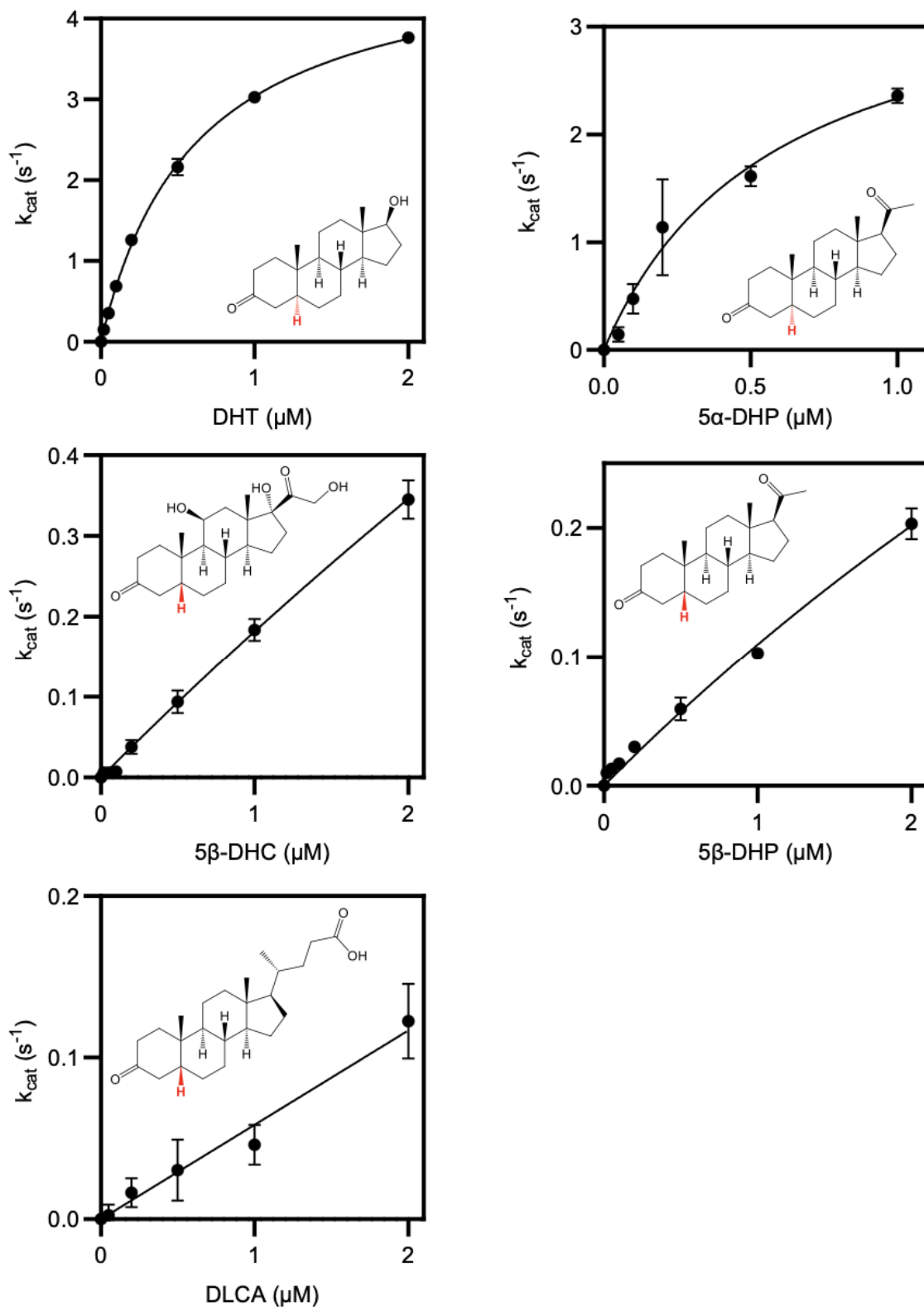
785
786
787
788
789

Extended Data Figure 2. Product of *C. steroidoreducens* HCS.1 incubation with progesterone.
Major progesterone product formed by *C. steroidoreducens* HCS.1. Comparison with reference standards confirms 3β-,5β-tetrahydroprogesterone (THP) production.



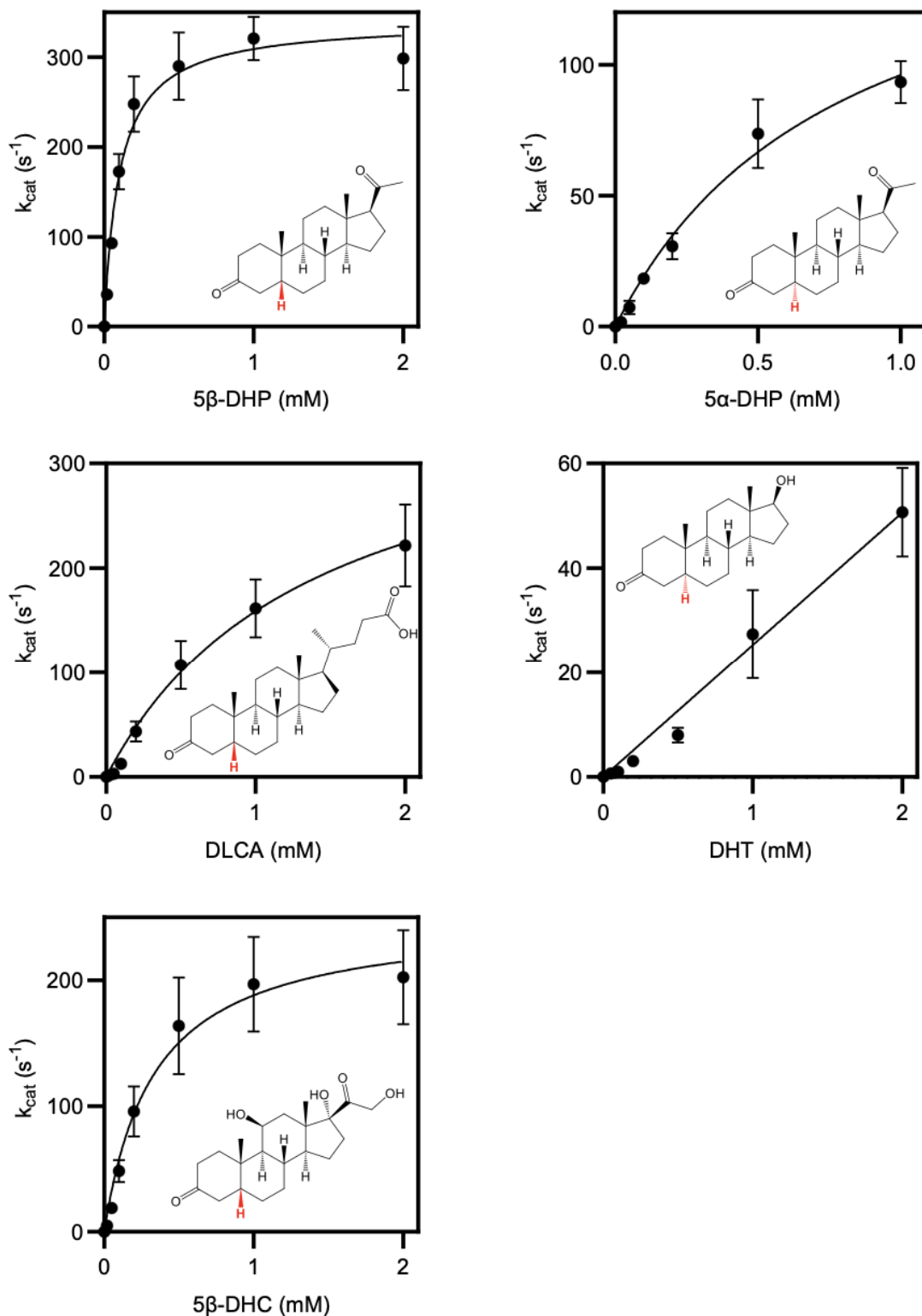
790
791
792
793
794
795

Extended Data Figure 3. 12% SDS-PAGE of *E. coli* lysates expressing SDR domain-containing proteins. SDS-PAGE analysis showing the heterologous production of *C. steroidoreducens* SDR domain-containing proteins in *E. coli*, pre- and post-isopropyl β -D-1-thiogalactopyranoside (IPTG) induction. Red boxes highlight expressed protein.

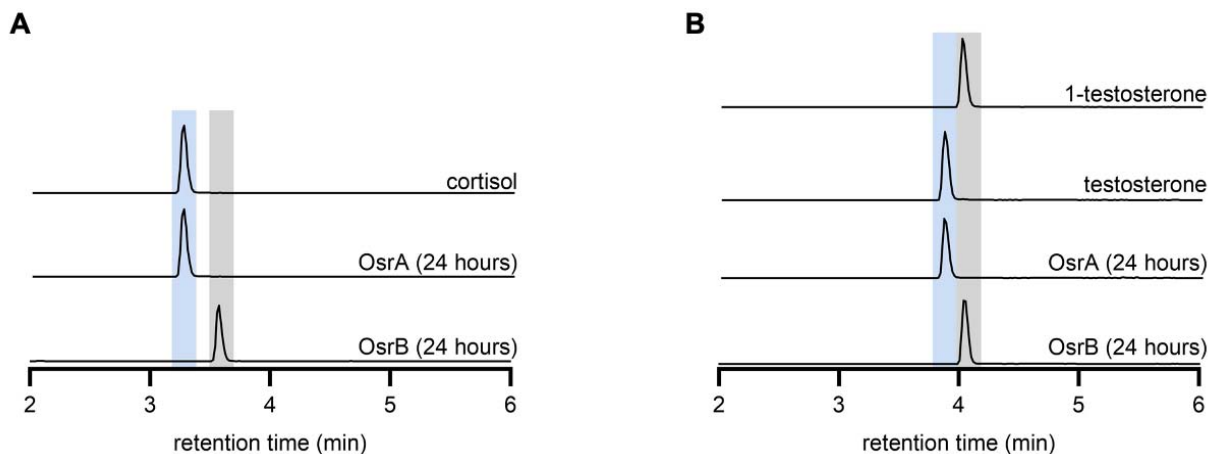


796
797
798
799

Extended Data Figure 4. Reaction rates of enriched BLEONJ_2554 on indicated substrates. Reaction rates for the 3'-reduction of 5-reduced steroids by anaerobically purified short-chain dehydrogenase BLEONJ_2554.

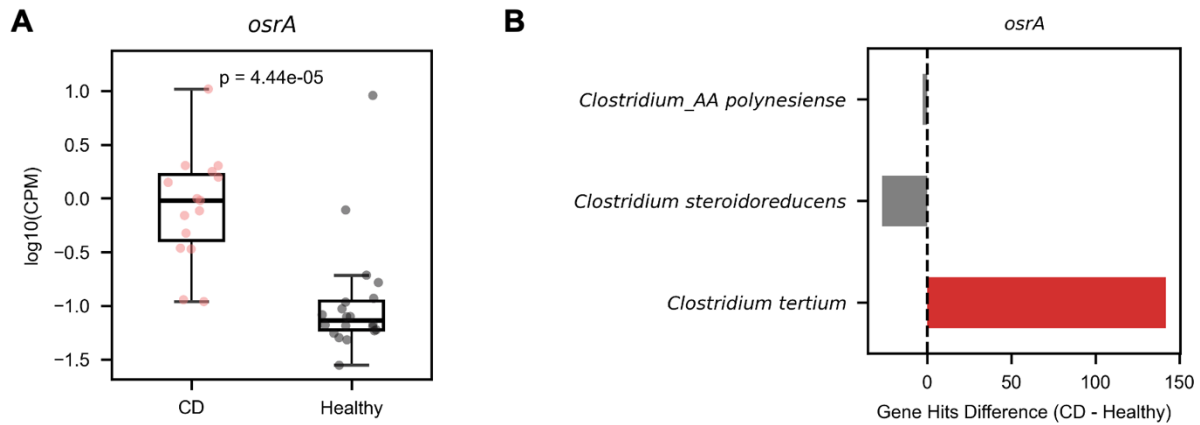


800
801 **Extended Data Figure 5. Reaction rates of enriched OsrC on indicated substrates.** Reaction rates
802 for the 3'-reduction of 5-reduced steroids by anaerobically purified short-chain dehydrogenase OsrC.



803
804 **Extended Data Figure 6. OsrA and OsrB products from Δ^1 - and Δ^4 -steroid hormone substrates.** (A)
805 Products following prednisolone incubation with purified OsrA or OsrB. Comparison with cortisol reference
806 standard confirm that OsrA generates the Δ^1 -reduced product and show that OsrB produces a distinct
807 cortisol isomer. (B) Products following boldenone incubation with purified OsrA or OsrB. Comparison to
808 reference standards confirm that OsrA and OsrB generate Δ^1 - and Δ^4 -reduced products, respectively.

809



810

811

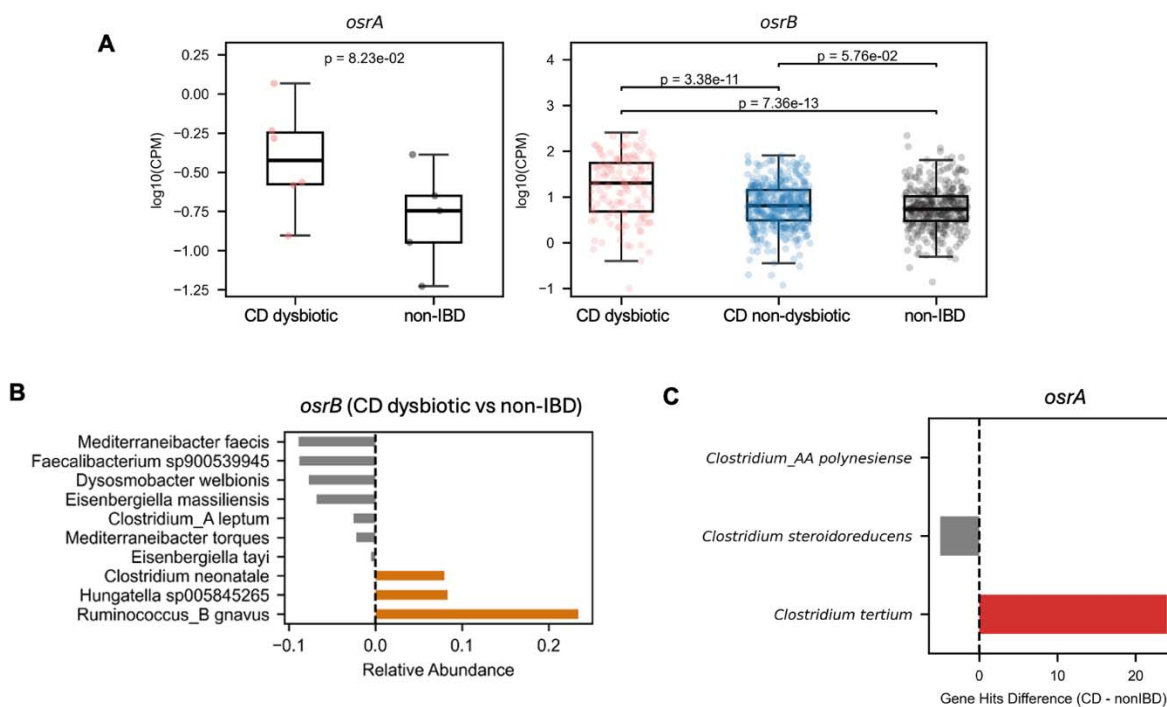
812 **Extended Data Figure 7. *osrA* levels in expanded dataset of healthy and Crohn's disease**

813 **metagenomes.** (A) Reads mapping to *osrA* homologs in expanded dataset of Crohn's disease (CD)

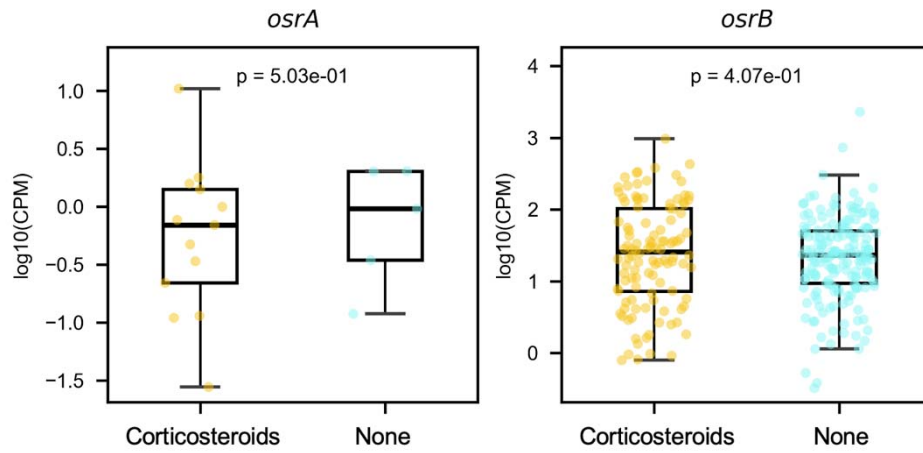
814 patient metagenomes relative to healthy controls. (B) Difference in *osrA* homolog levels in CD relative to

815 healthy metagenomes.

816



817
 818 **Extended Data Figure 8. Association between *osrA* and *osrB* and Crohn's disease in Integrative**
 819 **Human Microbiome Project metagenomes.** (A) Reads mapping to *osrA* and *osrB* homologs in Crohn's
 820 disease (CD) metagenomes relative to non-IBD controls. CPM stands for copies per million. (B)
 821 Difference in *osrB* homolog levels from taxa with the most significant changes in relative abundance
 822 between CD dysbiotic and non-IBD metagenomes. (C) Difference in *osrA* homolog levels in CD dysbiotic
 823 relative to non-IBD metagenomes.



824
825
826
827
828

Extended Data Figure 9. Association between *osrA* and *osrB* and steroid usage in the Lewis et al study. Reads mapping to *osrA* and *osrB* homologs in Crohn's disease (CD) patient metagenomes grouped based on patient corticosteroid treatment.